REVIEW OF THE ELECTRICAL COMMUNICATION LABORATORY
VOLUME 16, NUMBERS 9–10, SEPTEMBER–OCTOBER, 1968

U.D.C. 621.396.931.001.2

Field Strength and Its Variability in VHF and UHF Land-Mobile Radio Service

Yoshihisa OKUMURA, Eiji OHMORI,
Tomihiko KAWANO, and *Kaneharu FUKUDA*

Detailed propagation tests for land-mobile radio service were carried out at VHF (200 MHz) and UHF bands (453, 922, 1310, 1430, 1920 MHz) over various situations of irregular terrain and of environmental clutter. The results analyzed statistically are described for distance and frequency dependences of median field strength, location variabilities and antenna height gain factors for the base and the vehicular station, in urban, suburban and open areas over quasi-smooth terrain.

The correction factors corresponding to respective terrain parameters for irregular terrain, such as rolling-hill terrain, isolated mountain area, general sloped terrain, and mixed land-sea path are discussed.

As a result, a method is presented for predicting the field strength and service area for a given terrain of the land-mobile radio system, over the frequency ranges of 150 to 2000 MHz, for distances of 1 to 100 km, and for base station effective antenna heights of 30 to 1000 m.

The results of comparison of predicted field strength with measured data published in another paper suggests that a reasonable degree of accuracy is obtainable.

1 Introduction

VHF or UHF band mobile radios, especially for land use, have attracted attention as a means of police communication or as a prerequisite to full functioning of reporting services or traffic control by taxi companies. Indeed, there is every indication of their rapid growth as a new type of communication in the near future. Compared with the well-known propagation characteristics on the fixed radio syctem, that on the land-mobile service is burdened with peculiar complications. They are:

(i) The antenna height of a mobile body (mobile radio car) with which communication is held is very low—usually no more than 1 ~3m above ground.

(ii) Between the base station and the mobile radio cars or between such cars themselves, an ever changing, infinitely large number of propagation paths are formed due to movement from place to plce.

(iii) That causes the clearance of the propagation paths to be lost, while the field strength, hindered by the terrain irregularities and other obstacles, suffers great attenuation and location variability all the time,

In the meanwhile, sufficient test data has been reported on propagation characteristics connected with VHF and UHF band TV broadcasts, closely resembling those with land-mobile radio communication. This data has too many unknown elements to be applicable to the land-mobile radio be cause of peculiarities cited above.

For example, the propagation curves prepared by CCIR,[1] TASO,[2] and others are mainly intended for TV broadcasts with the antenna height fixed at 10m, but do not account for determining characteristics of antennas lower than that or for attenuatton due

to various terrain irregularities. On the other hand, for the land-mobile radio itself, some information such as propagation curve presented by J. J. Egli[3] and propagation test data reported by W. E. Young[4] is available; and, quite recently, CCIR has made a report on correction factor data[5] for antennas 3～10 m high. All these, however are not detailed enough to apply to this country where terrain is complicated and irregular.

In order, therefore, to obtain fundamental data for the design of land-mobile radios by clarifying the yet-unknown propagation characteristics, and to assure the possibility of introducing new frequency bands which will be much in demand, two series of experiments—one in 1962 and the other in 1965—were performed over the whole district of Kanto, inclusive of the heart of Tokyo. Four frequency bands were selected between 450 MHz～2000 MHz. All sorts of characteristics on attenuation and variation of the field strength were brough to light, both for quasi-smooth terrain and for hilly, mountainous, or otherwise irregular terrain full of obstructions.

Experimental reaults in UHF bands were added to the formerly obtained results[6] in a VHF band (200 MHz)—making up the land-mobile radio propagation design charts in the frequency ranges of 150～2000 MHz, transmission (base station) antenna heights of 30～1000 m, and distances of 1～100 km—the autors have found a method of predicting with fair exactitude the field strength for vaious sorts of terrain irregularities and environmental clutter.

This report is presented in the hope it will be of some use, and any criticisms will be greatly appreciated.

2 Outline of Propagation Tests Performed

2.1 Selection of Mobile Courses

(1) First Series of Tests

Time: November 1962～January 1963.

Topographicallv simple and flat areas were selected for these tests. Quasi-smooth terrains (the definition follows), which contained as many built-up cities as possible within a distance of 100 km were chosen and the transmission (base station) attennas were variable up to near 1000 m.

The mobile courses ran over the Kanto plains area, including the heart of Tokyo.

Care was taken to give two or more mobile courses for each base station, for a compara-

Table 1 (a) PATH CONDITION AND MOBILE COURSE IN FIRST PROPAGATION TEST

Transmitting Base Station	Trans. Ant. Height h_{ts}/h_{tg} (m)	Name of Mobile Course	Direction of Trans. Ant. Beam	Average Ground Level Over Course h_{ga}(m)	Effective Trans. Ant. Height h_{te}(m)	Situation of Path Terrain
Top of Mt. Tsukuba	848/35	Tachikawa	SW 50°	20	828	Quari-smooth terrain, urban, suburban, open area
		Tokyo	SW 30°	25	823	
Halfway of Mt. Tsukuba	239/6	Tachikawa	SW 50°	20	219	
		Tokyo	SW 30°	25	214	
Upper Floor of Tokyo Tower	246/228	Mito	NE 42.5°	10	236	
		Kumagaya	NW 24°	25	221	
Lower Floor of Tokyo Tower	156/138	Mito	NE 42.5°	10	146	
Marunouchi Tokyo	63/60	Soka	In the city of Tokyo	3	60	Nikko-Road
		Funabashi		3	60	Keiyo-Road
		Asaka		33	30	Kawagoe-Road
		Tamakawa		33	30	Tamakawa Road

tive study of attenuation and variations differing from one another according to the courses to be followed. Table 1 (a) shows particulars about such courses, base stations, propagation path situations, etc.

(2) *Second Series of Tests*
Time: March~June 1965.
This set of tests was carried out to make the results of the first series of tests more exact, aiming further at explaining the characteristics of lower base station antennas and some peculiarities concerning hilly, mountainous, or otherwise irregular terrain as well as investigating the interference characteristics of the waves. The mobile courses selected are shown in Table 1(b).

Figures 1(a) and (b) are roughly-drawn

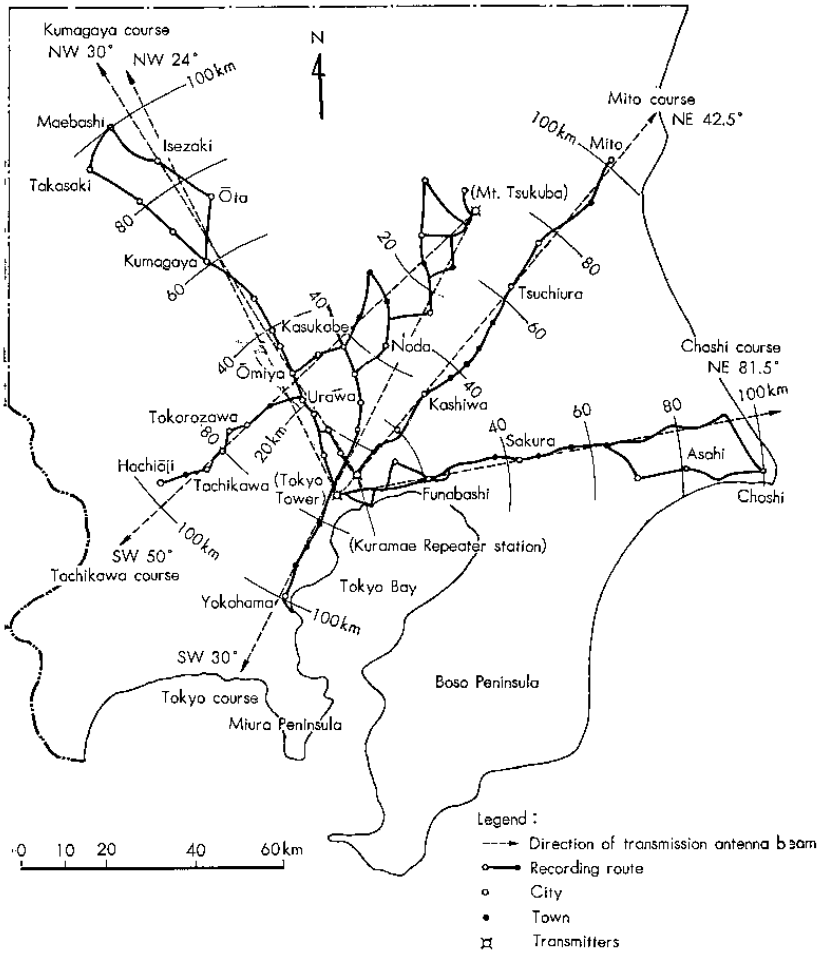

Fig. 1(a)—Map of Kanto District in Japan showing radials and mobile-recording routes over quasi-smooth terrain.

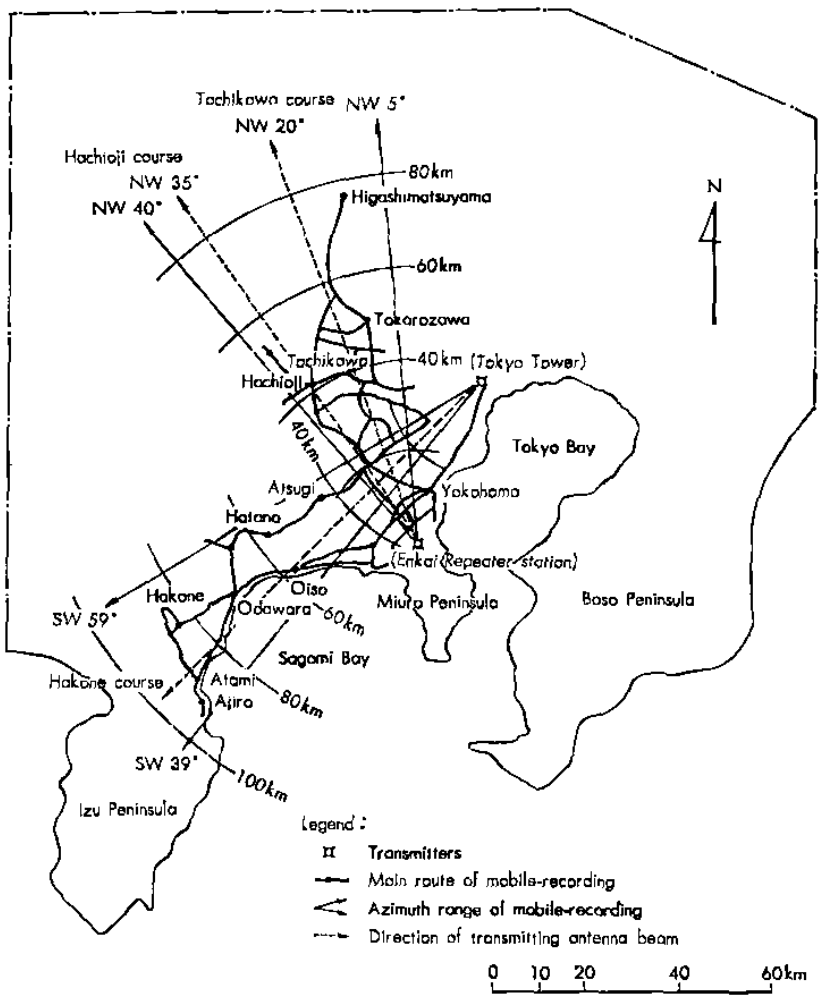

Fig. 1(b)—Map showing radials and mobil-recording routes over hilly and mountainous terrain.

maps of the Kanto district representing the mobile courses shown in Tables 1(a) and (b) respectively. The principal recording routes (built-up cities) are also indicated on them.

2.2 Frequencies; Parameters of Equipment used

The following frequencies were selected to find how they affect various characteristics; also to see if there was any possibility of developing new frequency bands:

First tests: 453 MHz, 922 MHz, 1310 MHz, 1920 MHz.

Second tests: 453 MHz, 922 MHz, 1317 MHz, 1430 MHz.

The vertically polarized wave was in use for all frequencies. Table 2 shows parameters of measurement with respect to the transmitter power, transmitting and receiving

Table 1 (b) PATH CONDITION AND MOBILE COURSE IN SECOND PROPAGATION TEST

Transmitting Base Station	Trans. Ant. Height, h_{ts}/h_{tg} (m)	Name of Mobile Course	Direction of Trans. Ant. Beam	Average Ground Level Over Course h_{ga}(m)	Effective Trans. Height h_{te}(m)	Situation of Path Terrain
Lower Floor of Tokyo Tower	150/132	Mito	NE 42.5°	10	140	Quasi-smooth terrain
		Choshi	NE 81.5°	5	145	
		Hakone	SW 45°	30	120	Hilly and mountainous terrain
Kuramae Relay Station	62/59	Mito	NE 42.5°	10	52	Quasi-smooch terrain
		Kumagaya	NW 30°	20	42	
Enkai Relay Station	163/9	Hachioji	NW 35°	55	108	Hilly and mountainous terrain
		Tachikawa	NW 20°	55	108	

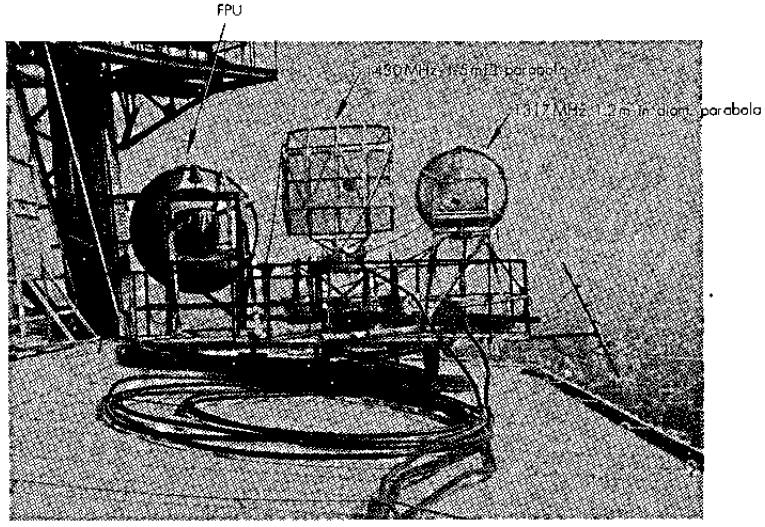

Fig. 2(a)—Transmitting antennas at Tokyo Tower.

antenna type and gain, etc., for all frequencies.

Figures 2(a) and (b) are photographs of the transmitting antennas installed at Tokyo Tower and Enkai transmitting base station, respectively.

2.3 Mobile Field Strength Measuremet

(1) Vehicular Station Antenna Height

The receiving annennas for all frequencies 3m high above ground, were installed at both sides on top of the mobile radio van, as shown in Fig. 3, to take normal measurements. Simultaneously with it, since most

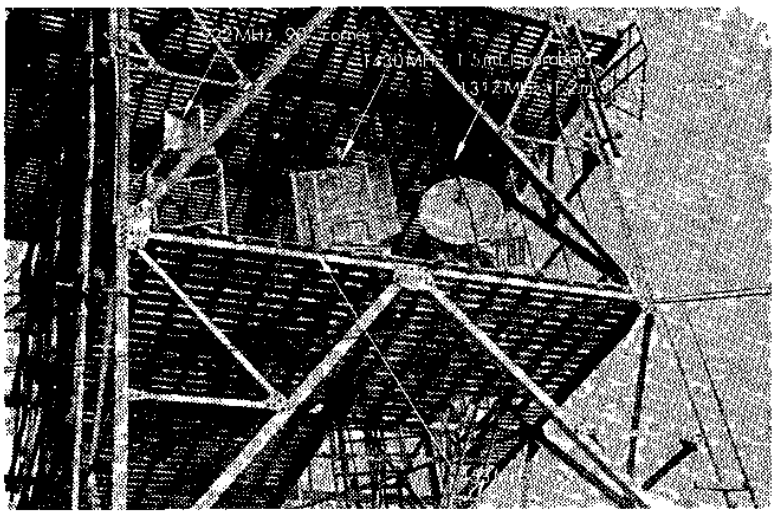

Fig. 2(b)—Transmitting antennas at Enkai base station.

Table 2 PARAMETERS OF MEASUREMENT

Frequency MHz	Transmitter Power	Transmitting Antenna Gain Type	Receiving Antenna Gain Type
453	150 W	11.3 dB 5-element Yagi	1.5 dB Omni-directional unipole antenna
922	60 W	11.5 dB 90° Corner	1.5 dB 〃
1317	150 kW Pulse	22.0 dB 1.2 m in diam. parabola	1.5 dB 〃
1430	30 W	26.3 dB 1.5 m parabola	1.5 dB 〃
1920	60 W	19.0 dB Horn	1.5 dB 〃

Note: Antenna gain is the value referred to the isotropic.

mobile radio cars have antennas lower than that, measurement was also taken with 1.5 m high antennas for a comparative study of vehicular station antenna height gain factors.

(2) Data Recording

The input signals from the antennas of the mobile measurement van, were led into their respective field strengh meters classified by frequencies, and the outputs therefrom recorded simultaneously, parallel and continuously, by a 4-pen recorder; if necessary, a magnetic tape recorder was made use of at the same time. The variation of received field strength produced by terrain irregularities and environmental clutter, was, as a rule, continuously put on record while traveling.

Special notice was taken of the variation of the median and the instantaneous signal level, with suitable adjustment made to the traveling and the recording paper speed. In

Fig. 3—Mobile field strength measurement van.

normal mobile recording, the variation of the median level due to terrain irregularities and environmental clutter was given more importance; and the traveling speed and the recording paper speed averaged 30 km/hr and 5 mm/sec respectively. In the case of instantaneous level variation, the method of sampling recording for a small sector of 50 m or so, was resorted to when passing through some prominent terrain irregularities and environmental clutter areas. The traveling speed and the recording paper speed this time averaged 15 km/hr and 250 mm/sec, respectively. The recorder pen action was so planned that it might exactly follow speedy variation caused by frequencies and so that the envelope in instantaneous variation might perfectly be separated. The minimum input level recordable was -125 dBm (-12 dBμ) for all frequencies, and the recorder scope was almost lineally 50 dB.

(3) *Obtaining Data*

The transmitting antennas beam was not wide enough for higher frequency bands, so the measurement car excluded regions where the corrected ratio of antenna directional characteristics became indistinct. Also, within about 10 km, like the built-up areas in the heart of Tokyo, horizontal omni-directional antennas were used for transmission as occasion demanded.

The field strength of the signal received by a mobile measurement car differs with the car running parallel to the direction of the incoming wave (along the path) or perpendicular to it (across the path). Therefore, in obtaining data, the measurement cars traveled on the roads not only in the direction of the main recording routes shown in Fig. 1, but in all directions, especially in the central parts of cities and towns.

2.4 Expressing Propagation Characteristics

Some propagation curves hitherto published were not definitive, because they took in all sorts of elements of terrain irregularities and environmental clutter haphazardly so were not very useful for estimating field strength or service area adapted to the real situation.

It might be better to refer here to the manner of terrain feature classification, and to treatment and expression of various data observed in performing this study.

(1) *Classification and Definition of Terrain Features*

There are an infinite variety of terrain features on this earth. But our basic idea is that the "quasi-smooth terrain" should be the standard of analysis and expression of propagation characteristics.

By the "quasi-smooth terrain" is meant a flat terrain where, judging from the propagation path terrain profile (drawn from a map on the scale of 1 : 50,000), the undulation height is about 20m or less with gentle ups and downs and, moreover, the average level of ground does not differ much (not more than 20m). The Kanto plains meet these requirements on the whole.

Other terrains are difined as "irregular" and are divided into "rolling hilly terrain,"* "isolated mountain," "general sloping terrain," and "mixed landsea path."

Besides the classification of terrains, the following are definitions of the path and the terrain parameters, as well as the differentiation method used here.

(a) Base Station Effective Antenna Height

To obtain a field strength suitable for any existing terrain, it is necessary to define the antenna height of the base station. In the terrain profile shown in Fig. 4, let the average level of ground within 3 to 15km (or less if the entire distance does not exceed 15km) from the base station antenna be h_{ga}, the base station antenna height be h_{ts} above sea level; then the effective transmitting antenna height will be defined as $h_{ts}-h_{ga}=h_{te}$. The antenna height gain factor will be examined at this height.

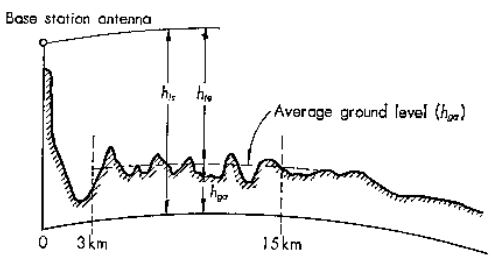

Fig. 4—Definition of effective transmitting antenna height (h_{te}).

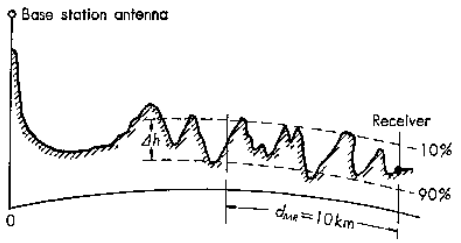

Fig. 5—Definition of the parameter (Δh, "terrain undulation height") for rolling hilly terrain.

(b) Terrain Undulation Height (Rolling Hilly Terrain Parameter Δh)

Almost all propagation paths have irregular undulations. In a rolling hilly terrain, the "terrain undulation height Δh" expressing the degree of irregularities, may be found from Fig. 5 equal to the difference between 10% and 90% of the terrain undulation height (as the profile shows) within a distance of 10km from the receiving point to the transmitting point.

This manner of determining terrain parameters may apply to a mountainous area where there are several mountains which affect the receiving point by multiple diffraction, but not to a simple sloped terrain or where there is only one undulation.

(c) Isolated Mountain Ridge and Path Parameter

When the propagation path has a single mountain in the way and there is nothing else to interfere with the receive signal except the obstacles in the neighborhood, the mountain is defined as an "isolated mountain." Such a mountain is presumed to be approximate to a knife edge, when the VHF and UHF band are in use.

Figure 6(a) shows the path parameter of an isolated ridge whose height h is measured from the average ground level.

Figure 6(b) shows a model of an isolated ridge where attenuation is calculated from a

* Mountainous terrain determination method involves correction for the rolling hilly terrain.

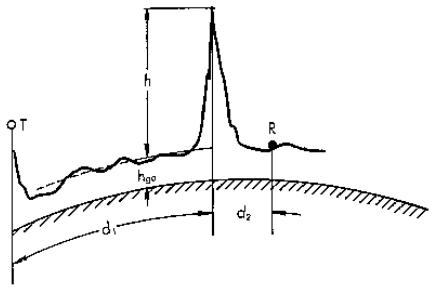

(a) Path parameter

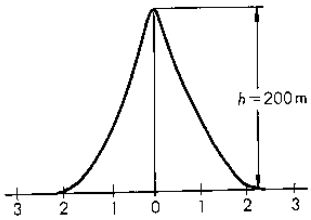

(b) Model

Fig. 6—The model and geometrical parameter of isolated ridge.

standard height $h=200$ m. Proportional attenuations may be obtained by conversion for other heights.

(d) Average General Slope Angle of Terrain (θ_m)

When terrain, whether flat or undulated, slopes over a distance of at least 5 to 10 km, the terrain parameter in terms of the average angle of general slope θ_m may be expressed, as is shown in Fig. 7, by

$$\theta_m=\frac{h_n-h_m}{d_n}$$

where, if $h_n>h_m$ (uphill), the slope angle is positivive $(+\theta_m)$ and if $h_n<h_m$ (downhill), it is negative $(-\theta_m)$.

(e) Distance Parameter for Mixed Land-Sea Path.

Where there is an expanse of sea or lake in the propagation path, three different cases are presumable. Figure 8 shows where the

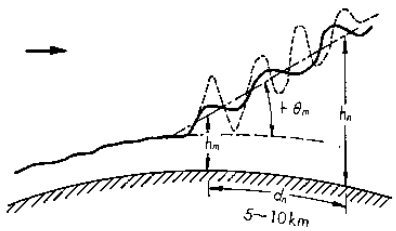

(a) Positive slope $(+\theta_m)$

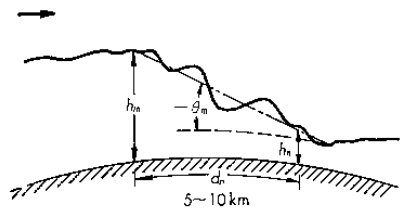

(b) Negative slope $(-\theta_m)$

Fig. 7—Definition of average angle of general terrain slope.

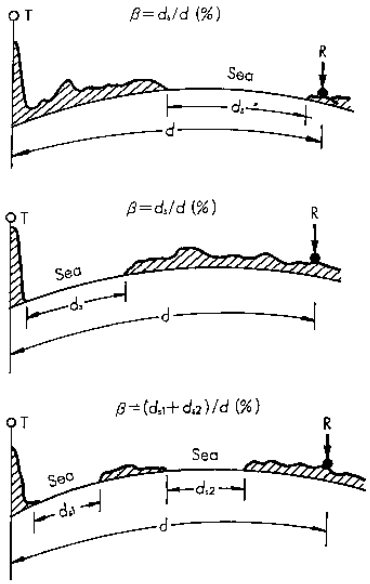

Fig. 8—Definition of distance parameter (β) for mixed land-sea path.

exapanse of water is (a) near the mobile radio car, (b) near the base station, and (c) midway between. Thus three distance parameters usable as terrain parameters may be obtained.

(2) *Classification and Definition of Environmental Clutter*

Whether in a quasi-smooth or an irregular terrain, buildings and trees near the mobile radio car antennas affect the received field strength in diverse ways, according sort and condition of such buildings and trees. In fact, such obstacles in all individual areas classified into minute groups in pursuit of propagation characteristics, would be of little practical use, because that would only make finding the mobile radio field strength in a given area more difficult. Instead, let the ground obstacles be examined in the following three groups classified according to the degree of congesting and shielding:

(a) Open Area

In which are classed an open space where there are no obstacles like tall trees or buildings in the propagation path and a plot of land which is cleared of anything 300 to 400 m ahead, as, for instance, farm-land, rice-field, open fields etc.

(b) Suburban Area

This comprises a village or highway scattered with trees and houses—the area having some obstacles near the moblile radio car, but still not very congested.

(c) Urban Area

This is a built-up city or large town crowded with large buildings and two-or-more-storied houses, or in a larger village closely interspersed with houses and thickly-grown tall trees.

(3) *Treatment of Data; Method of Expression*

All the received field strength data recorded throughout by the mobile van were treated statistically. That is, for each of the classified areas defined above, the entire distance was divided into "sampling interval" 1 to 1.5 km each, and readings taken the so-called "small-sector medians" at intervals of about 20 m. Thus was found the cumulative distribution in that sampling interv—alone of the objects of analysis. And to the attenuation of the field strength due to terrain irregularities and environment clutters, was given the median value of the distribution curve described above (or the sampling-interval median); also to the location variability was given the variation range (e.g., the standard deviation) of the distribution. In expressing the field strengths affected in various ways by terrains and other obstacles, the standand was determined by the urban field strength median in a quasi-smooth terrain (called the "basic median field strength" or simply "basic median"). Then followed the steps to obtain the difference between this standard and the median actually measured for each of the above-classified terrain features, that is to say, the correction factor, positive or negative. And these correction factors were obtained by determining the relation with respective terrain paramerers.

The reason the value for urban area paths was selected as the standard instead of the value (more usually turned to account) under simpler conditions as, for instance, in open or suburban area paths, is explained here. It has been known from experiment that, of all the classified terrains and obstacles, it is in fact in the suburban area that the field strength suffers the most multifarious variations, especially when the receiving antenna height is low. Also, in Japan, there are few areas virtually satisfying the open area conditions; and if any, they ara narrow. The urban area, on the contrary, is best-situated in definitely judging the effects of obstacles, and has conveniences of getting more data in comparatively a small space. The highest degree of accuracy may be expected of the standard value it provides.

3 Propagation Characteristics on Quasi-Smooth Terrain

3.1 Field Strength Variation while Traveling

In land-mobile radio service the vehicular antenna height is extremely low. While the car is in motion, an infinite number of propagation paths are formed between itself and

the base station; and its received field strength is subject to multifarious location variations, which are caused by the obstacles coming up one after another in and around the path or by the standing waves due to the inteference of multi-path waves. The following is an outline of how the field strength varies:

(a) There is, in a large swelling variation of the average field strength level, overlapping each other, a deep instantaneous variation of quick periodic motion, due to the changes in terrain irregularities and environmental clutter.

(b) The average field strength level (sampling-interval median), when viewed from the median attenuation relative to free space, has the largest value in the urban area followed by suburban and open area. For instance, even within the same distance, when the car moves from an open area into an urban area, there occurs a change of as large as 20 to 30 dB. The dynamic range of changes in a 20 km radius are amounts to no less than 50 to 60 dB according to the existing obstacles.

(c) Since, behind the obstacles, the overlapped field strength level variation reffered to in (a) crosses the standing waves due to the multi-path diffracted or the multi-path reflected waves, the variation depth becomes very large—almost equal to the Rayleigh distribution. The speed of variation increases

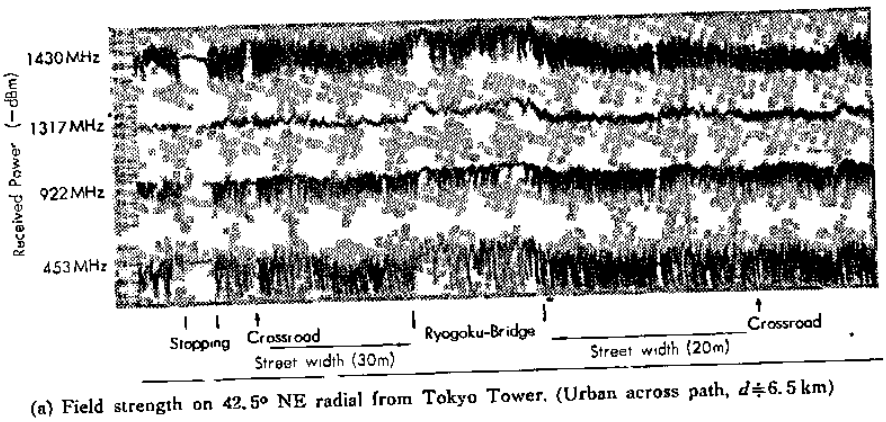

(a) Field strength on 42.5° NE radial from Tokyo Tower. (Urban across path, $d \fallingdotseq 6.5$ km)

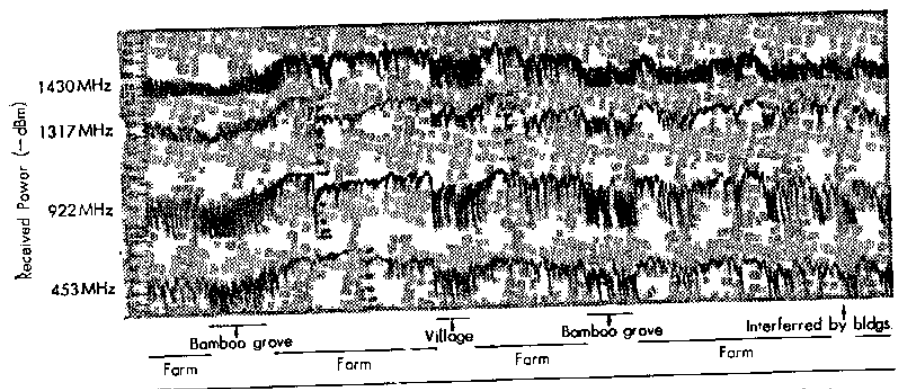

(b) Field strength on the Atsugi-road from Enkai station. (Rural, oblique path, $d \fallingdotseq 25$ km)

Fig. 9—Examples of amplitude recording of the received field strength.

in proportion to the product of the frequency of the radio wave and the traveling speed. So a position change of only a few meters by the car, will produce a sharp change of 10 to 20 dB in the field strength.

Figure 9 shows examples of amplitude recording of the received field strength, indicating how it undergoes variation at frequencies of 453 MHz, 922 MHz, 1,317 MHz (pulse), and 1,430 MHz. Figure 9(a) is the record made on an oblique course in an urban area (crowded with 3 to 5-storied buildings and other houses) near Ryogoku, about 6.5 km from Tokyo Tower base station. No marked changes in the average levels can be seen for all frequencies, except that on Ryogoku Bridge there is a rise of about 10 to 15 dB.

Figure 9(b) is the record made on the Atsugi Road, about 25 km from Enkai base station, while traveling obliquely in the direction of the incoming signal. The average level of variation while traveling is very large —within about 25 dB, as this is a suburban area where various obstacles are mixed together on both sides of the road, like farm lands, groups of houses, buildings, etc.

Thus the manner in which the field strengh changes while traveling is vague and uncertain. It may therefore be understood that, in land-mobile radio service, it is more practical to obtain in a statistical manner the attenuation at sampling intervals based on roughly-classified obstacles according to their nature and situation, than to pursue the value in each individual spot.

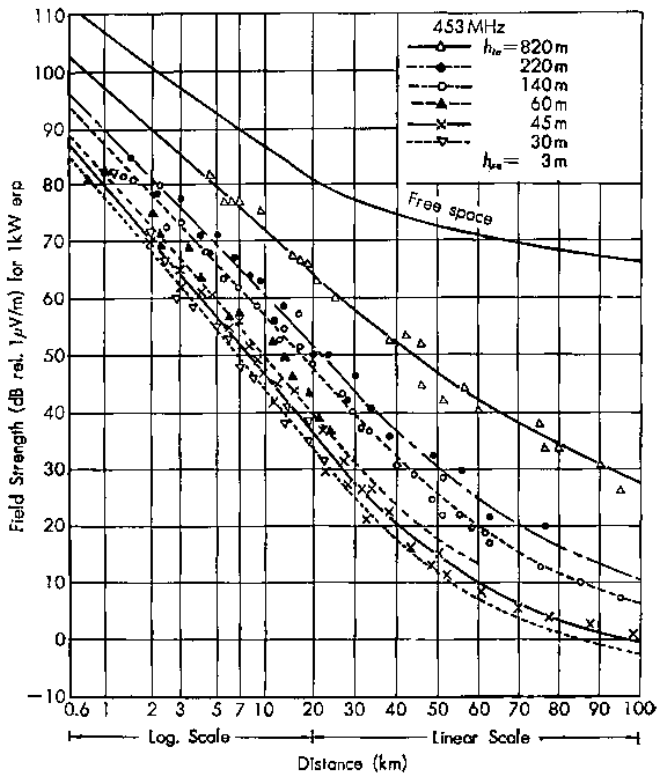

Fig. 10 (a) 453 MHz

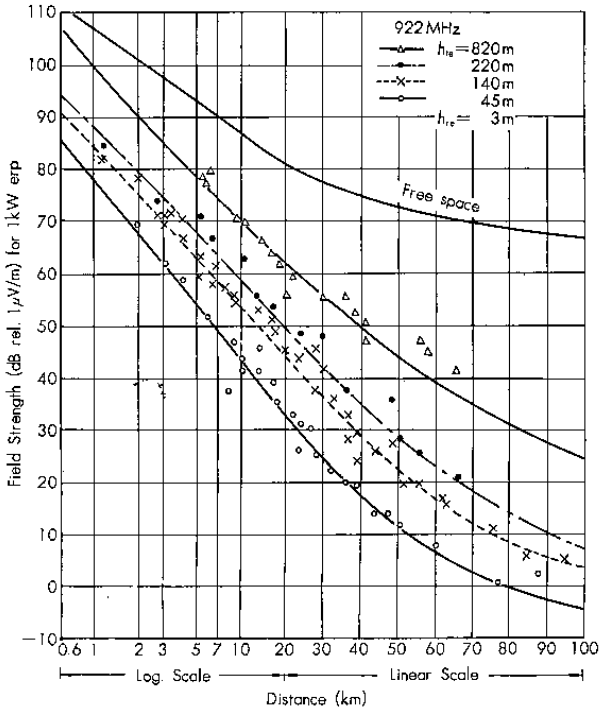

Fig. 10 (b) 922 MHz

3.2 Field Strength Attenuation Characteristics with 3 m High Receiving Antenna

3.2.1 Distance and Frequency Dependence of Field Strength in Urban Area

(1) Median Field Strength vs. Distance Curves at Various Frequencies

Figures 10 (a) to (e) represent the median field strength (dB rel. 1μV/m for 1 kW e.r.p.) versus distance data, measured in urban areas at 453 MHz, 922 MHz, 1,317 MHz, 1,430 MHz, and 1,920 MHz. In this experiment on quasi-smooth terrain, the transmitting antennas are of five different heights ranging from 62 to 848 m above sea level, but their effective heights (h_{te}) on the average are 820 m, 220 m, 140 m, 60 m, 45 m, and 30 m, though there may be differences of some few meters according to the course. Measurement data was analyzed on the basis of these effective antenna heights. Also the measured values in relation to the distances are shown plotted with averages of the medians of sampling-intervals, each of approximately the same distance, situated in the same urban area. These measured values mean nothing but the averaged values for various directions—along-the-path, across-the-path, etc.,—of traveling in the urban area. The median field strength thus obtained in the quasi-smooth terrain urban area, tends to show a comparatively smooth change with distance, for each base station antenna height and for each frequency. The curves in Fig. 10 are so drawn as to show this smooth change. Now let various charactertstics be investigat-

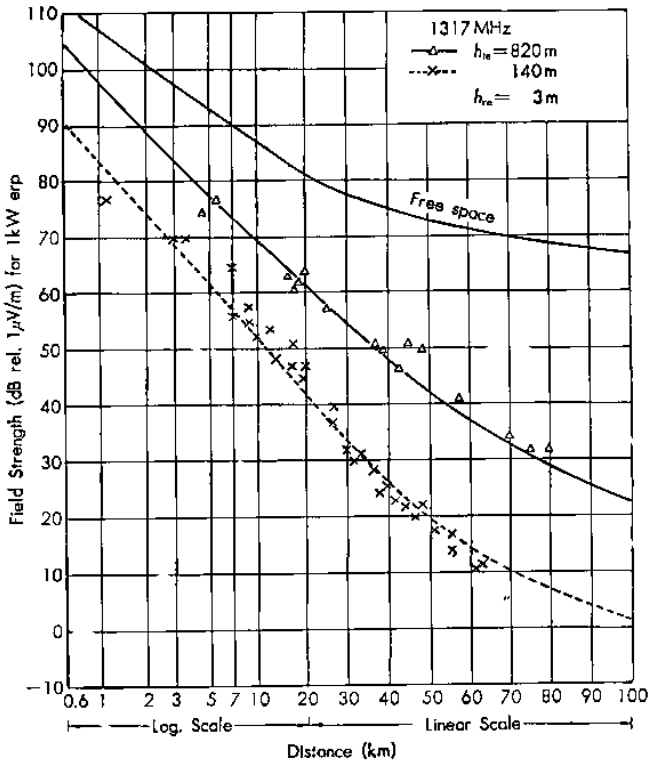

Fig. 10 (c) 1,317 MHz

ed on the basis of these smoothed curves.

(2) *Distance Dependence of Median Field Strength in Urban Area*

The distance dependence of the field strength is one of the fundamental problems of propagation. From the measured data shown in Fig. 10, this distance dependence develops somewhat different tendency according to the frequency and the effective antenna height of the base station. Figure 11 shows the distance dependence in terms of the median attenuation relative to free space, when the base station antenna effective height h_{te}=140 m and the frequencies are 453 MHz, 922 MHz, 1,430 MHz, and 1,920 MHz. The median attenuation goes on to increase within distance of about 15 km, by about the distance to the one half-th power ($A \propto d^n$, $n \fallingdotseq 1/2$, where A; median attenuation, d: distance). For over 15 km, a sudden increase follows, but within 40 to 100 km it remains a constant rate, showing $n \fallingdotseq 2.3$. The distance dependence represented in the relation of the median field strength (E_m) to the base station antenna effective height (h_{te}), will give n ($E_m \propto d^{-n}$) as is shown in Fig. 12. When the distance is less than 15 km, the value of n becomes smaller as h_{te} grows higher (Curve A); and when 40 km $< d <$ 100 km, the maximum value of $n (n \fallingdotseq 3.3)$ appears in the neighborhood of $h_{te} \fallingdotseq 200$ m, while n decreases when $h_{te} \fallingdotseq 70$ m or less (Curve B). It may be said also that, with a low h_{te}, the field strength lapse rate is small (or the long-distance dependence is gentle); and in a middle distance (where 15 km $< d <$ 40 km), n takes on intermediate value between Curve A and Curve B in Fig.

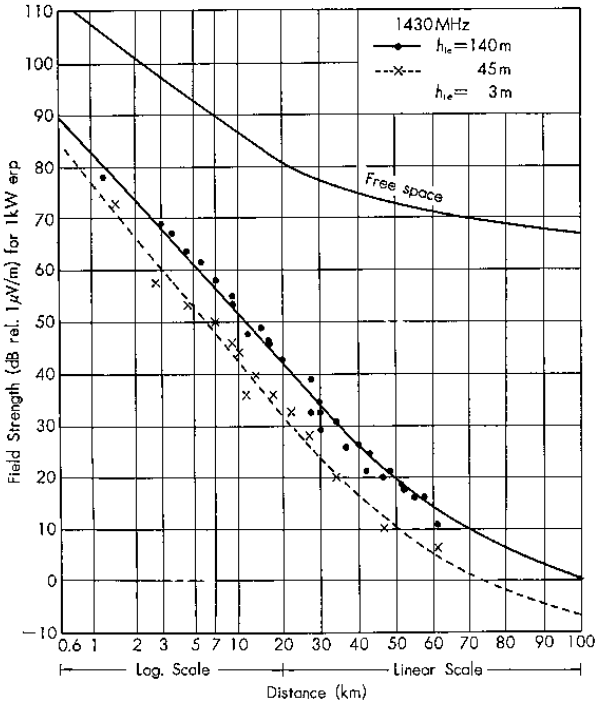

Fig. 10 (d) 1,430 MHz

12. Unless the distance is broken into small divisions, however, n does not remain constant.

(3) *Frequency Dependence of Median Field Strength in Urban Area*

On a quasi-smooth terrain the field strength attenuation is largest in the urban area, and it increases as the frequency becomes higher. Figure 13 shows the frequeney dependence of median attenuation relative to free space in an urban area, at h_{te}=140 m for example, where the value for 453 MHz is taken as the standard. This dependence in terms of the field strength lapse rate relative to frequency ($E_m \propto f^{-n}$), is shown by the curves for n in Fig. 14. The values of n vary according to the frequency band and distance; let the frequency bands—100～500 MHz, 500～1,000 MHz, 1,000～2,000 MHz—be taken, then the higher the frequency the larger the value of n; it also grows large as the distance increases.

In J. J. Egli's prediction curves[8] which incorporate some terrain factors into plane earth calculation, the characteristic shows a constant value of $n=0(E_m \propto f^{-n})$ for the whole range of 40～1,000 MHz and it differs to a considerable degree compared with the values of n in Fig. 14. Figure 15 shows the prediction curves depending on distance and frequency, which represent the median attenuation relative to free space (called the "basic median attenuation") in a quasi-smooth terrain urban area, where the base station effective antenna height h_{te}=200 m and that of the mobile radio car h_{re}=3m. These curves, from which the basic median field strength is predictable, derive themselves from the curves (in Fig.

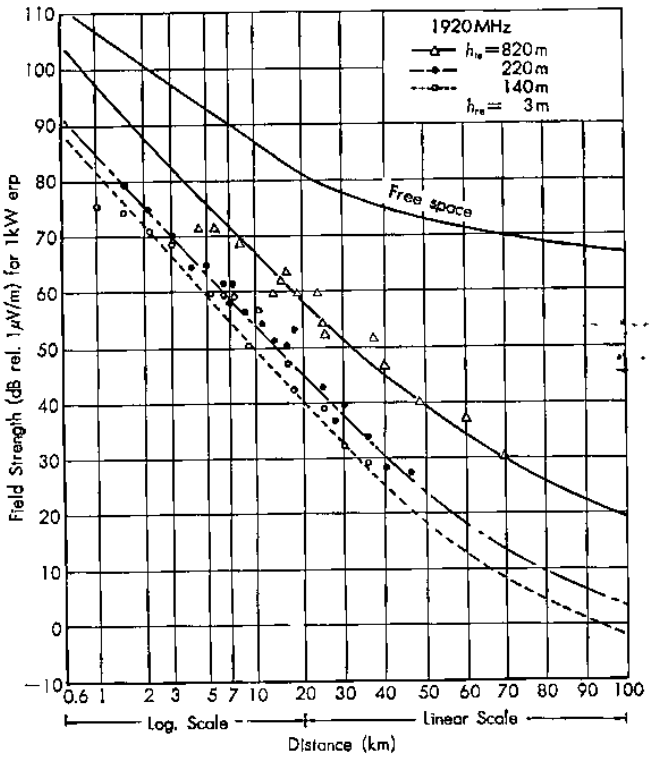

(e) 1,920 MHz

Fig. 10—Examples of median field strength data in urban area for various effective antenna heights (453 MHz).

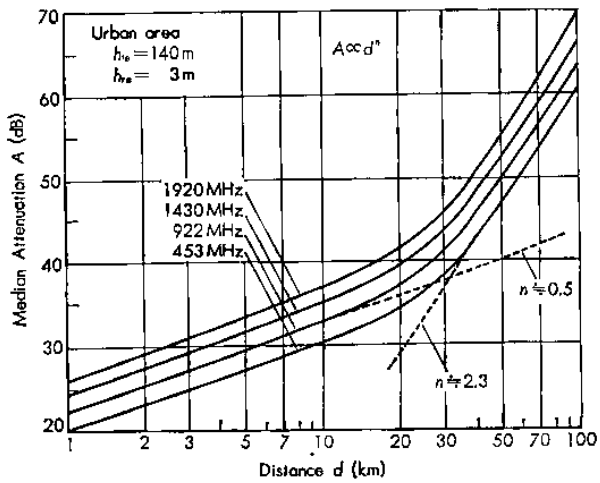

Fig. 11—Example in distance dependence of median field strength attenuation in urban area.

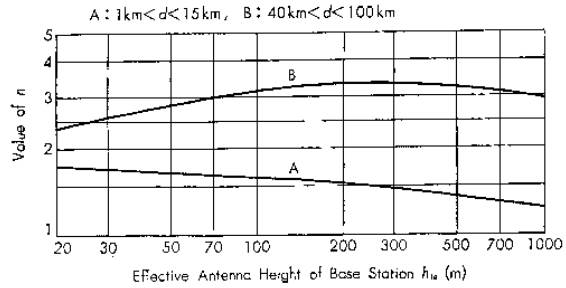

Fig. 12—Distance dependence of median field strength in urban area ($E_m \propto d^{-n}$).

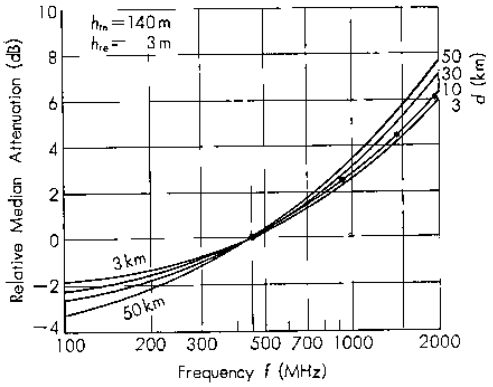

Fig. 13—Example of frequency dependence of median attenuation relative to free space in urban area.

10) which, plotted with distance as a parameter, denote the median field strength data measured at different frequencies, with reference to the base station effective antenna height and the median attenuation relative to free space, by interpolating h_{te}=200 m. For the VHF band, the results[6] from an experiment formerly made at 200 MHz are also employed.

3.2.2 Median Attenuation in Urban Area in Relation to Vertical Angle of Arrival

The field strength median attenuation in highly built-up urban area, depends on such variables as the mean height of the buildings,

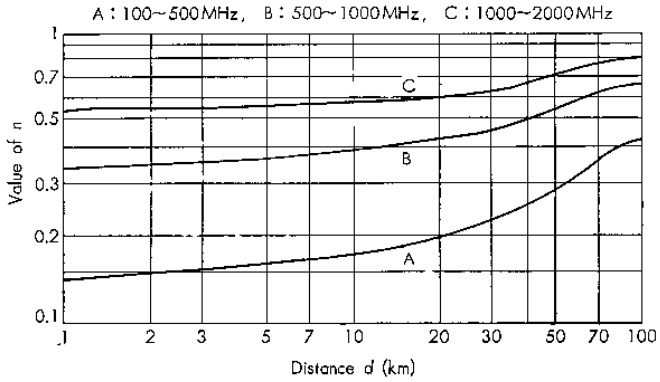

Fig. 14—Frequency dependence of median field strength in urban area ($E_m \propto f^{-n}$).

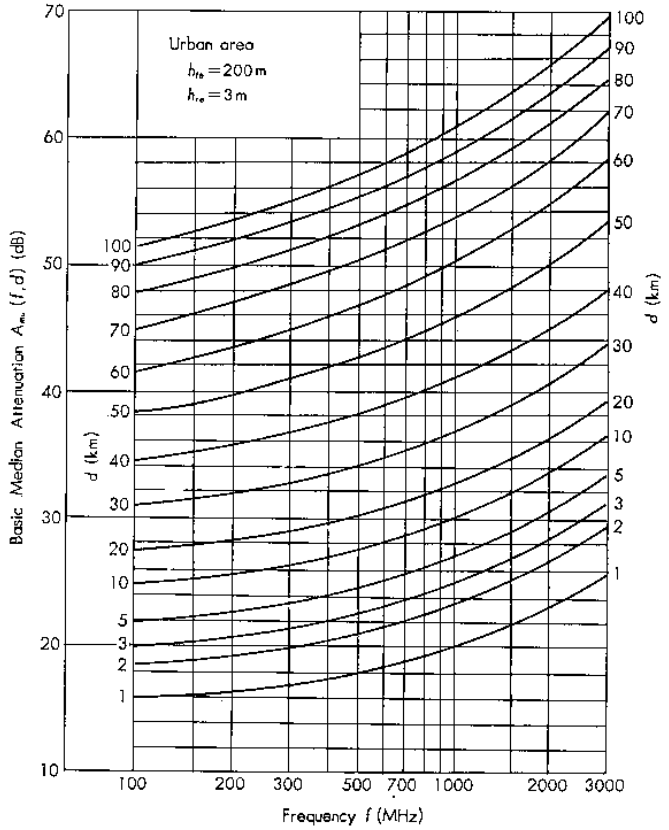

Fig. 15—Prediction curve for basic median attenuation relative to free space in urban area over quasi-smooth terrain, referred to h_{te}=200 m, h_{re}=3 m.

mean width of the streets, vertical angle of arrival of the signal from the base station antenna, and also the direction of travel with regard to the direction of the incoming signal. The relation to the vertical angle of arrival (that is, the elevation angle the base station antenna forms with the mobile radio car) is also connected with the base station antenna height and the distance. In examining this problem, reference will have to be made to the results of an experiment[7] recently conducted in Italy.

The Italian experiment states that the vartically polarized waves (146 MHz, 475 MHz) transmitted from the mobile radio car equipped with an antenna 2 m high, were received at several points, to find the relation of the vertical angle of arrival to the median attenuation relative to free space, each traveling interval being 500 to 1,000 m on various streets with different kinds of buildings. Curve A in Fig. 16 represents the result based on a vertical angle of arrival ($\alpha°$)=4°. The distance range is not indicated in this experiment; but it may probably have been within 2 to 3 km. Curve B in Fig. 16 shows the result from our own data within this range.

Curve B relates to the case where the distance was made variable while the base

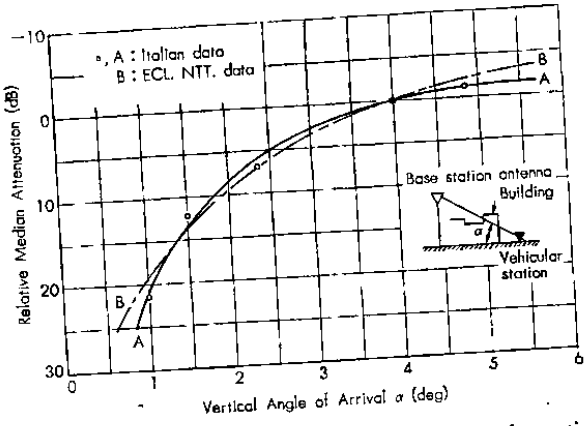

Fig. 16—Dependence of the additional attenuation on the vertical angle of arrival (attenuations are referred to 4°).

station antenna height kept constant, and it well corresponds with the Italian Curve A.

3.2.3 Difference of Median Attenuation due to Orientation of Urban Street

Generally, the received field strength changes according to how the road on which the car travels is oriented with regard to the direction of the signal. Especially in urban areas, clear disparity in median attenuation presents itself, according to whether the course is parallel (along the path) or perpendicular (across the path) to the direction of the signal; the width of the road, too, has more or less effect upon it. Figure 17 shows, in mean values, how along-the-path median attenuation differs from across-the-path median attenuation in the urban area, in respect of various distances and frequencies. Note that the larger the distance the smaller the difference. The median attenuation differences at 453 MHz averages 9 dB for 10 km and 6.5 dB for 50 km. As there is not much difference due to frequencies, from the "basic median" the prediction curves for the along-the-path and the across-the-path correction factor, are obtainable as shown in Fig. 18.

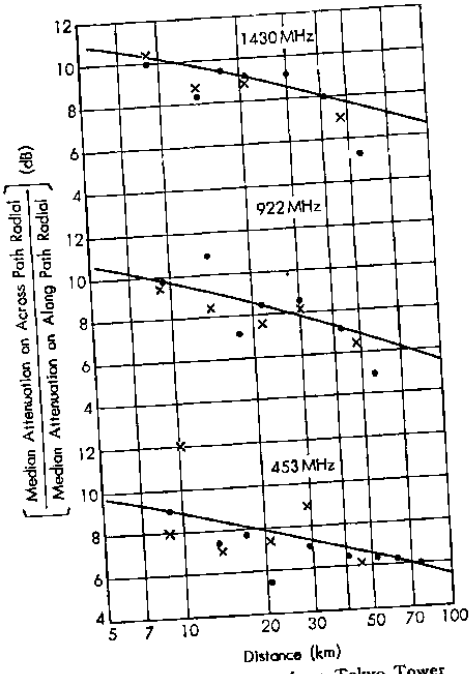

• h_{te}=140 m Mito course from Tokyo Tower
× h_{te}= 42 m Kumagaya course from Kuramae

Fig. 17—Difference of attenuation in urban area due to the orientation of the street with respect to the radius starting from the base station.

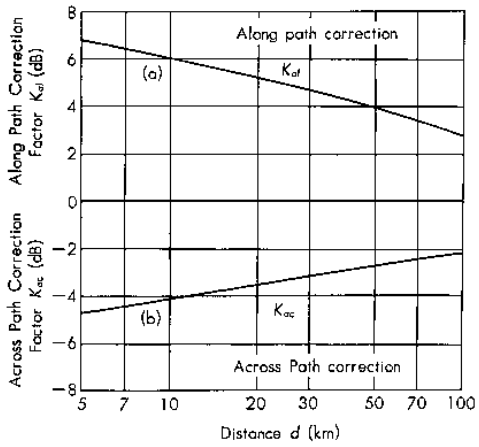

Fig. 18—Prediction curves for along and across path correction factor in urban areas.

3.2.4 Medinn Attenuation in Suburban Area (Suburban Correction Factor)

In suburban areas, the degree of congestion and shielding due to obstacles is slighter than in urban areas; and there the median field strength is usually high. Not specifically drawing the distance dependence curves of field strength for suburban areas, the authors tried to obtain the "suburban correction factor," which is the difference between the median attenuation (or median field strength) in the urban area and that in the suburban area. Figure 19 shows this correction factor by frequencies measured at various distances. There seems to be no great difference arising from the distance and base station antenna height. Therefore, supposing that the correction factor in constant for the whole distance, its mean frequency dependence indicates 8.5 dB at 453 MHz, 10 dB at 922 MHz, and 12 dB at 1,920 MHz. In the light of this suburban area correction factor frequency dependence, connected with the urban median attenuation frequency dependence (shown in Fig. 15), it may be seen that, in the suburban area, the field strength within the frequency band 400 to 1,000 MHz yields no more difference than 1 dB. This is also the case with the CCIR

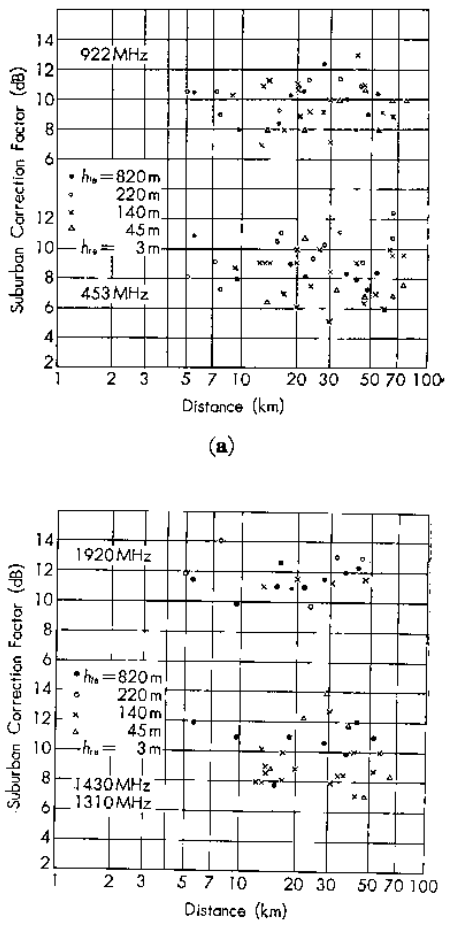

Fig. 19—Difference of median in urban and suburban area.

propagation curves.[1] From this result of measurement come the prediction curve representing the suburban correction factor frequency dependence shown in Fig. 20.

3.2.5 Attenuation in Open Area (Open Area Correction Factor)

The spaces that satisfy the conditions of open area are not to be found in too long sampling intervals. Stressing the check of

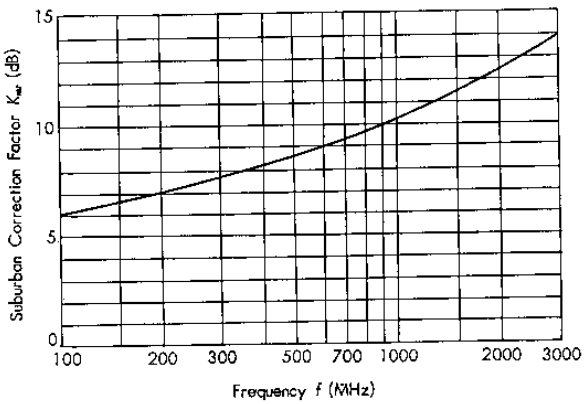

Fig. 20—Prediction curve for "suburban correction factor" as a function of the frequency.

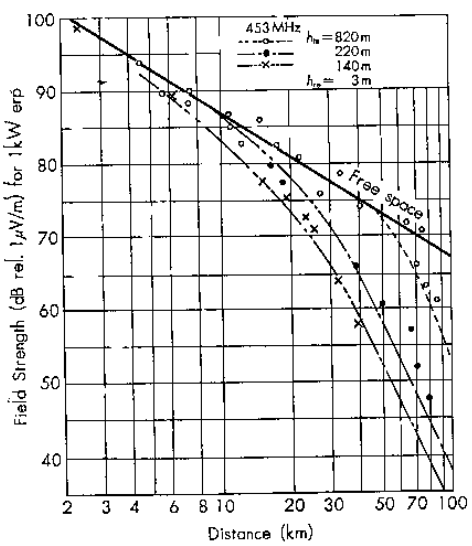

Fig. 21 (a) 453 MHz

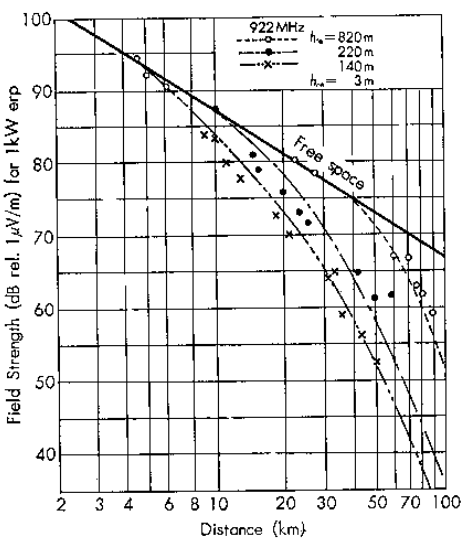

Fig. 21 (b) 922 MHz

received signal levels, propagation experiments obtained the quasi-maximum of field strength for analysis.

Figures 21(a) to (c) show the quasi-maximum of field strength plotted as a function of the distance. The curves represent its smoothed values. Attenuation begins to appear at about 5 km from the base station whose effective antenna height h_{te}=140 meters. A sudden increase in attenuation may be discerned for distances more than that.

When the quasi-minimum attenuation relative to free space that depends on the distance, is compared with the urban area

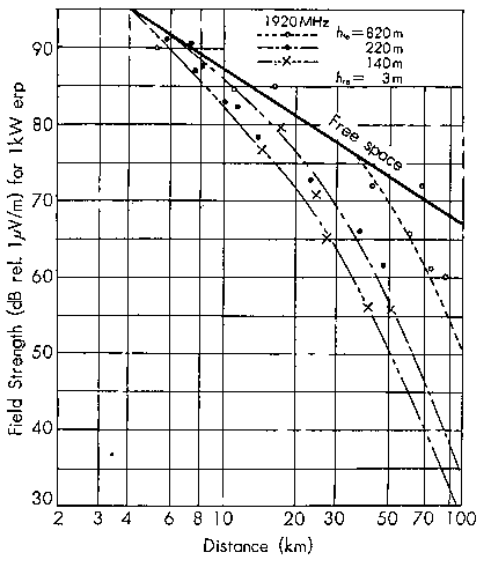

(c) 1920 MHz

Fig. 21—Examples of field strength (quasi-maximum) data in "open area" for various effective antenna height of base station.

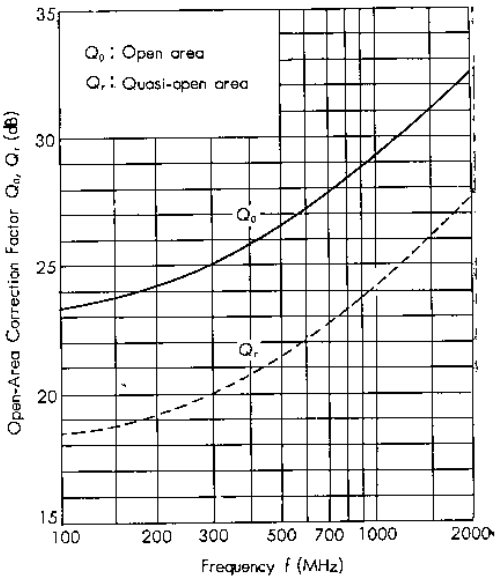

Fig. 22—Prediction curves of "open-area correction factor" as a function of the frequency.

median attenuation (the effective antenna height of the base station being the same), the differences are: 26 dB at 453 MHz, 29 dB at 922 MHz, and 32 dB at 1,920 MHz—all remaining constant on the whole regardless of the distance.

Curve Q_0 in Fig. 22 is the prediction curve of the correction factor, which is represented with the difference between the quasi-maximum of field strength in an ideal open area and the median field strength in an urban area (or "basic median"). But when the corrected field strength becomes higher than the free space value, in cases where the base station with a high antenna is in a short distance, the free space value should be taken. As referred to above, the spaces in which Curve Q_0 must be corrected are very scarce—only such particular places as midway between the open and the suburban area (tentatively called the "quasi-open area"). And in such an area the median field strength may be smaller by about 5 dB than the quasi-maximum strength in an open area. Curve Q_r in Fig. 22 is the prediction curve of the correction factor in a quasi-open area represented in the same way as that for Q_0. By this correction, the open area field strength remains nearly constant for all frequencies, as in a suburban area.

3.3 Relation between Antenna Height and Field Strength (Antenna Height Gain Factor)

While the base station antenna height is usually more than scores of meters, the vehicular station antenna is no higher than 1 to 3 m above ground. There are naturally functional differences between the two, which must be considered separately.

3.3.1 Base Station Antenna Height Gain Factor

According to the definition of base station antenna height (h_{te}) given for our experi-

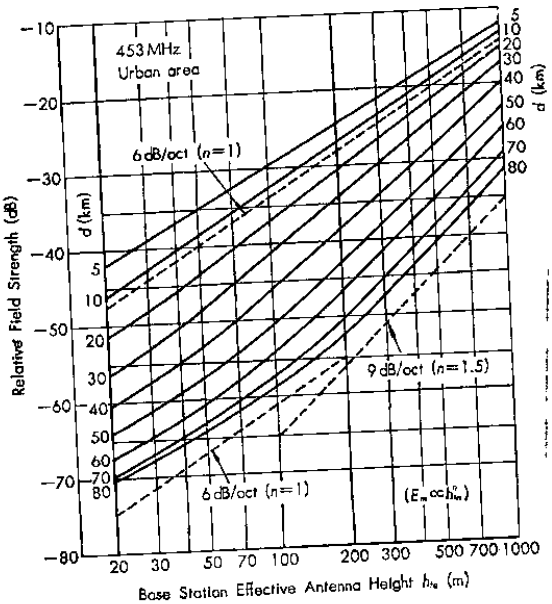

Fig. 23—Dependence of base station effective antenna height on median field strength in urban area.

ments, it may have six different heights—820 m, 220 m, 140 m, 60 m, 45 m, and 30 m. So let the gain factors be examined from the test results on each of them.

Figure 23 shows, at 453 MHz for example, the depeneence of the relative median field strength (or the reciprocal of the median attenuation) on the urban base station effective antenna height (found from the smoothed curves relating to measured distance dependence given in Fig. 10). The distance, as a parameter, is shown as 5~80 km. When the effective antenna height is 30~1,000 m and the distance is in the neighborhood of 10 km, the field strength tends to be linear uniformly at 6 dB/oct ($n=1$, $E \propto h_{te}^{n}$). It rises to 9 dB/oct ($n=1.5$) or thereabout with a high antenna at a long distance, it falls, with a low antenna, below 6 dB/oct, not necessarily showing a linear trend. This comes gradually when the base station antenna is low and the transmission path covers a long distance.

The tendency desribed above is the same with other frequencies. On the basis of all this, the prediction curves (shown in Fig. 24) have been obtained for the base station antenna height gain factor, with h_{te} fixed at 200 meters. These curves serve to predict the "basic median field strength."

3.3.2 Vehicular Station Antenna Height Gain Factor

(1) Relative Gain Factor for 1.5 m and 3 m

Figure 25 shows, for various frequencies and base station effective antenna heights, the differences of the medians in one and the same urban sampling interval measured, with a 3 m- and a 1.5 m high vehicular station antenna made exchangeable. There are slight fluctuations in the measured values; but they show no remarkable changes with respect to the distance and base station ef-

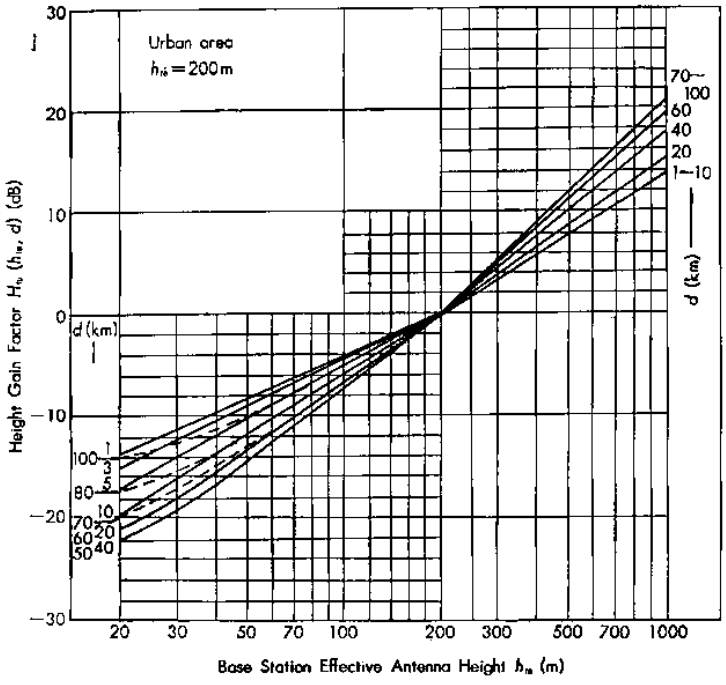

Fig. 24—Prediction curves for base station antenna height gain factor referred to h_{te}=200 m, as a function of distance.

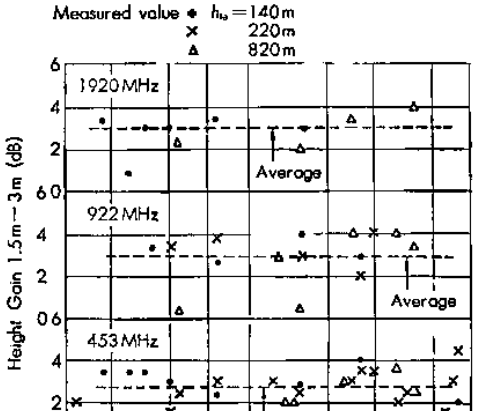

Fig. 25—Measured values of 1.5 m to 3 m height-gain of vehicle in urban area.

ective antenna height. On the average, the height gain is 3 dB for all frequencies as shown by the broken lines in Fig. 25.

It follows that the vehicular station antenna height gain factor for a height of 3 m or less, is supposed to be 3 dB/oct (n=1/2, $E \propto h_{re}^{n}$).

(2) Gain Factor for Height above 3 m

The vehicular station antenna height for land-mobile radio service may not usually be more than 3~4 m. However, the recently-developed super-highways in large cities, mostly 10 m or so above ground, have induced the authors to make an investigation on the antenn again factor for heights more than 3 m.

As a supplement to our propagation experiments, the results of measurement made at several fixed points are shown in Fig. 29. It may be known that the higher the frequency the larger the height gain, which

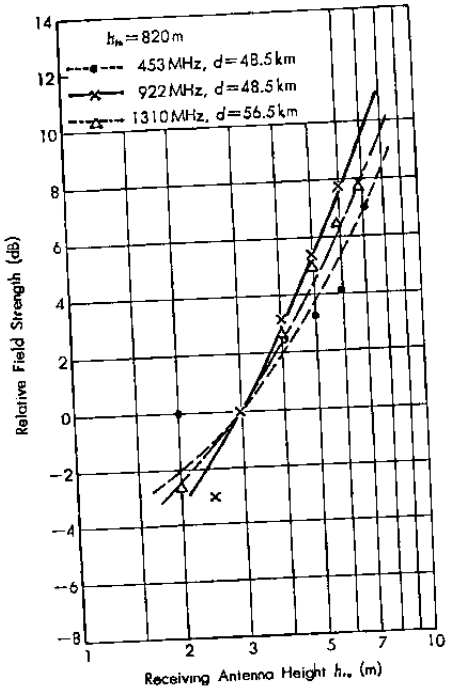

Fig. 26—Examples of height gain measurement of receiving antenna in urban area.

tends to be 6 to 8 dB/oct ($n=1\sim1.3$, $E\propto h_{re}{}^{n}$). As measured values are not ample enough to find the final gain factor, some more data will be referred to for further examination.

According to the height patterns measured by the NHK Technical Laboratory[8] at eight medium and small cities at frequencies of 87 MHz, 176 MHz, and 670 MHz, with the antenna height ranning from 4 to 10 m, the points of inflection appear in the neighborhood of 4 to 6 m; and there is a sharp linear inclination for more heights up to 10 meters.

The appearance of the points of inflection is probably related to the average height of the houses in Japanese cities being 5 m; and for heights more than that, the shielding effect of the houses becomes smaller. So the height patterns are presumed to take considerably different forms according to the average height of houses and buildings in a city. That is, in a built-up residential area (large city) where the building height averages more than 15 m, the points of inflection would move up to more than 10 m in the pattern curves, showing $n<1$ ($E\propto_{re}{}^{n}$) between 3~10 meters.

In this connection, the following data[9] on the relative gain factor for heights of 10 m and 3 m, are recently reported by CCIR:

Frequency band	Suburban area	Large city
450~1000 MHz (Band IV, V)	6~7 dB ($n\fallingdotseq0.7$) (dependent on Δh)	4~5 dB ($n\fallingdotseq0.5$)
30~250 MHz Band III	7 dB ($n\fallingdotseq0.78$)	4~6 dB ($n\fallingdotseq0.5$)

There is another report of the measurement[10] taken in the heart of Tokyo, recently issued by the NHK Technical Laboratory confirming that the value is about 6 ~7 dB.

The prediction curves for vehicular antenna height gain factors in a medium-small and a large city, in cases where the antenna height is variable from 1 to 10 m (standard 3 m), if drawn on the basis of all the foregoing data obtained, would be as shown in Fig. 27. These curves will be of use for the prediction of the basic median field strength, and also for the conversion of antenna height gains needed for a comparative study of other propagation curves.

4 Propagation Characteristics on Irregular Terrain

4.1 Correction Factor of Field Strength on Rolling Hilly Terrain

The terrain parameters are to relate the degree of terrain irregularities with the field strength. Where the vehicular antenna height is no more than a few meters, there are several ways to decide them; and the most representative ones so far published are: the CCIR,[11] TASO,[12] and Thiessen[13] method. They are mostly intended for 10 m high TV receiving antennas and have their merits and

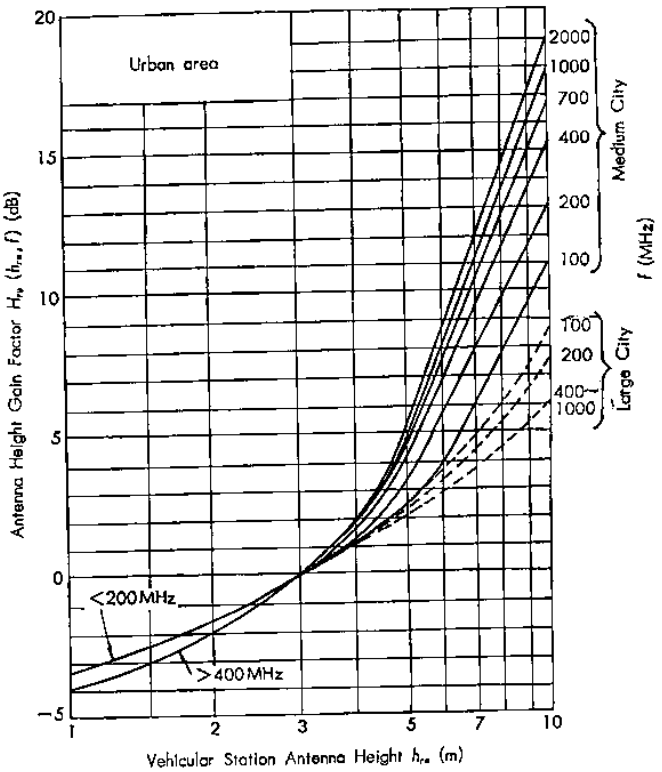

Fig. 27—Prediction curves for vehicular antenna height gain factor in urban area.

demerits, because some are not very clear in description; others are strict in description but must go through complicated processes.

If the receiving antenna is fairly high (more than 10 m), the strict description has enough meaning of its own; but where the vehicular antenna is as low as 1 to 3 m and the field strength suffers a change of more than 10 dB under the influence of houses and trees near it, the description will have to loss the bulk of its meaning.

To find, therefore, a correction factor for field strength in a sampling interval for mobile radio service with as much ease and promptitude as possible, let this method of deciding terrain parameters be based on the following:

(i) To obtain the terrain undulation height Δh following the definition given in Section 2.4, (1), (b), and the method suggested in Fig. 5. This coincides with the description of the CCIR method, but the interval originally intended is 10 km ahead of the receiving point.

(ii) To apply this Δh to undulations of more than a few in number. It is replaced by another parameter (average angle of general slope θ_m), when the place is a simple general sloped terrain.

(iii) To resort, in addition, to a measure of fine correction, when the vehicle happens to be on top or at the bottom of an undulation, in order to find a proper relation between Δh and the correction factor. This means that the correction for the rolling hilly terrain is subjected to treatment from two sides—the sampling interval median and the

fine correction adapted to the terrain undulations—which is suggested by F. H. Wise.[14]

(1) *Sampling Interval Correction Median on Rolling Hilly Terrain*

The data used for this analysis are taken from those measured by a mobile radio car while traveling on Tama rolling hilly terrain, the signals mostly transmitted from the Enkai base station. The values of Δh may be found from the profiles drawn for each azimuth angle of 1° relative to the traveling region. The additional median attenuation was analyzed with the difference between the

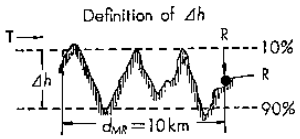

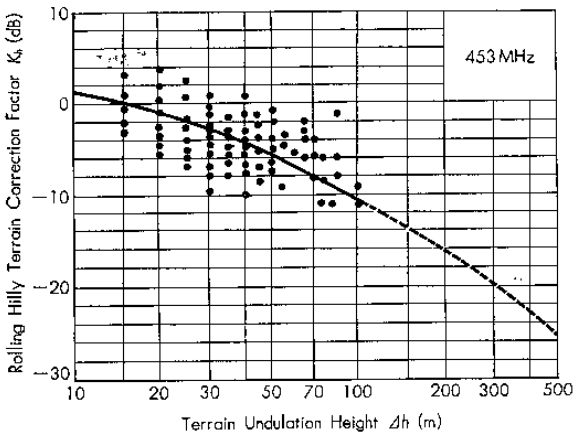

Fig. 28(a) 453 MHz

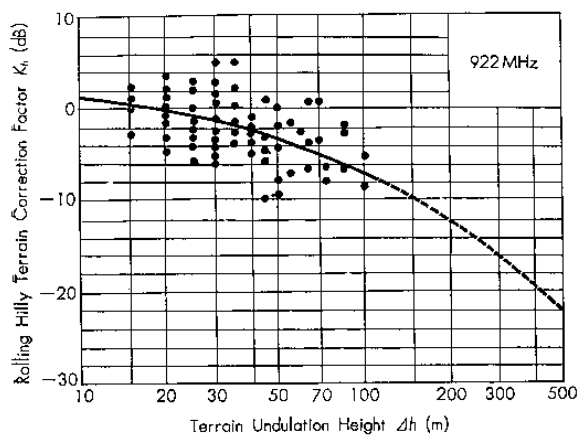

Eig. 28(b) 922 MHz

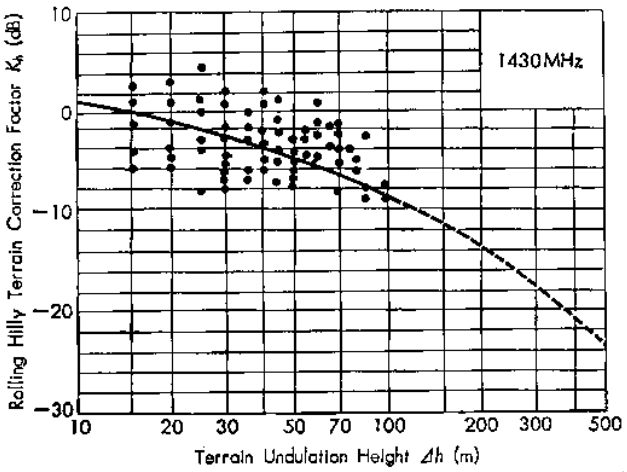

(c) 1430 MHz

Fig. 28—Measured values and prediction curve for "rolling hilly terrain corretion factor."

two values—the sampling interval median of field strength in the rolling hilly terrain and the median field strength (or basic median) for a distance equal to the aforesaid interval in the quasi-smooth terrain urban area (the base station effective antenna height being kept the same), and then this value was represented as a function of the undulation height Δh.

Figures 28(a) to (c) explain how Δh is related to the additional median attenuation (or rolling hilly terrain correction factor), respectively, at 453 MHz, 922 MHz, and 1,430 MHz. The correction factor relative to Δh is seen fluctuating conspicuously for all frequencies, becoming larger as Δh increases. The full-line cuves are smoothed curves for the factor. As no measured values of Δh above 100 m are available, the curves representing them are drawn with refrence to the CCIR curves.

The characteristics tend to be the same with each of the three frequencies; but the correction factor dependence on Δh at 922 MHz, at region of a large Δh, is found to be about 3 dB smaller than that for 453 MHz, and a point midway between the factors for 1,430 MH.

(2) *Fine Correction Factor on Rolling Hilly Terrain*

The correction factor dealt with in the precediug section (1) relates to the sampling interval median taken while the mobile van is just rising up from the bottom of an undulation.

If, on a rolling hilly terrain, the mobile van draws very near an undulation, the attenuation rises far above the correction factor referred to in the preceding section. On a course rather close to the top of the undulation, it falls below the factor, with the field strength ascending in the meantime.

The analysis that follows is concerned with the fine correction factor (that is, the factor adjusting once again the correction factor referred to in the preceding section), while the mobile van is traveling on a road lying at bottom or on top of an undulation. Figure 29 shows a maximum of changes ($\pm$dB) from the correction factor referred to in the preceding section, or the rolling hilly terrain fine correction factor as a function of the terrain undulation height Δh. The schematic diagram appearing above the curve is to give an idea of the field strength variation correction relative to the terrain profile.

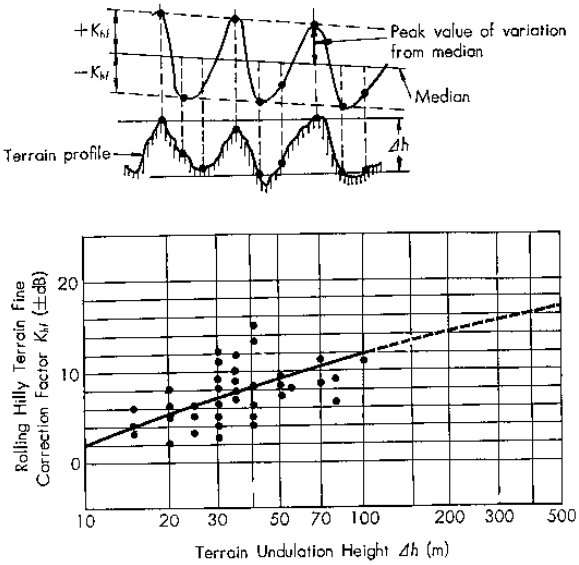

Fig. 29—Measured values and prediction curve for "rolling hilly terrain fine correction factor."

In a position at the bottom of the undulation which is on the side of the base station or on a road lying within 100 m from the side of the undulation, it would be well to correct the correction factor ($-K_h$) of Fig. 28 first and ($-K_{hf}$) of Fig. 29 next; while, on top of the undulation, the sum of the two factors ($K_{hf}-K_h$) would have to be corrected.

(3) *Vehicular Station Antenna Height Gain Factor on Rolling Hilly Terrain*

In the same way as for an urban area (Fig. 25), Fig. 30 shows the vehicular antenna height gain factor relative to the frequency and distance on a rolling hilly terrain, in other words, the differences of the medians in one and the same sampling interval measured, with the antenna height made changeable from 3 m to 1.5 m. Some fluctuations can be seen in the measured values, but there seems to be no distinct variation with respect to the distance. On the average, the gain factor is found to be 2.8 dB at 453 MHz, 3.3 dB at 922 MHz, and 3.3 dB at 1,430 MHz, showing no great difference among them. Hence estimation of the antenna height gain factor for heights below 3 m on a rolling hilly terrain to be 3 dB/oct.

4.2 Correction Factor for Isolated Mountain

Where the propagation path makes its way through mountains rising one above another, the rolling hilly terrain correction factor would in most cases be capable of prediction. But if there is an isolated mountain ridge like a knife edge, it must be dealt with differently. There are several ways of treatment intended for 10 m high TV receiving antennas suggested so far.

Originally, the calculated value of knife-edge diffraction is to indicate a loss relative to the free space value. When the receiving antenna is low, even though the ridge top is in a free space range against the base station, the received field strength behind the ridge usually suffers more loss than the

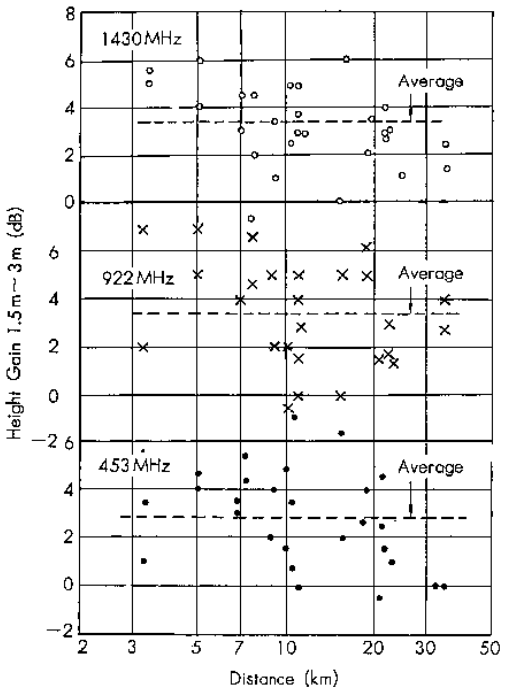

Fig. 30—Measuured values of 1.5 m to 3 m height-gain of vehicular station in rolling hilly terrain.

free space value minus the knife-edge diffraction loss.

Goldsmith[15] and Epstein,[16] in their treatment of this point, both introduce Norton's theoretical values and experimental factors as expressing the additional loss. Wise,[14] on the other hand, tries to obtain the value of field strength without resorting to this action, but acts promptly by deducting the correction factor relative to the basic CCIR curves. This may be said to be a simple method in a practical sense.

This paper likewise puts more stress on methods of practical use. So the basic idea is to find the correction factor relative to the basic median, by using an adequate terrain parameter, following substantially the Wise method.

Figure 31 shows, when the freqency band is 450~900 MHz and the isolated ridge height $h=100\sim350$ m, the deviation of the measured median field strength from the basic median, with the ridge height correction factor normalized at $h=200$ m, for each of the distance ranges 10~20 km, 20~40 m, and 50~70 km, against the distance from the ridge top d_2. Curves A, B, and C represent smoothed prediction curves for the respective mean distances. In normalizing the ridge heights, measured correction factors (in dB) were multiplied by α by means of the following empirical formula:

$$\alpha=0.07\sqrt{h}, \qquad h:(\text{meters}). \qquad (1)$$

This conversion factor is given in Fig. 32.

From the findings above, it may be seen that the field strength becomes higher than the basic median on the ridge top, the correction factor approximates 0 in a position a little way down the top (back distance $d_2<1$ km), and the attenuation shows its maximum most probably at the base of the ridge where $d_2\fallingdotseq2$ km or so.

Now examine the method where by the isolated ridge correction factor (Fig. 31) depends on the back distance d_2, comparing with the knife-edge diffraction calculation.

Curve B in Fig. 33 represents Curve B at $d_1=30$ km in Fig. 31 just as it is, while Curve K shows the calculated value of knife-edge diffraction loss for d_2 at 450 MHz, $h=200$ m, $d_1=30$ km. The two curves are drawn so as to show their correlation by causing 0 dB graduation (for Curve B) on the left and 20 dB graduation (for Curve K) on the right to come on the same level, assuming that the terrain factor of the basic median (like experimental factors referred to before) is 20 dB. In examining these curves together, a comparatively well-coincided tendency may be seen so far as $d_2>2$ km; but the loss on Curve K in increases if $d_2<2$ km, because of the fact that the isolated ridge model has a thickness while the knife-edge model has none, thus bringing about, as a matter of course, a difference between the two curves. Furthermore, the magnitude of knife-edge diffraction loss is practically independent of d_1 as long as h is constant, and does not

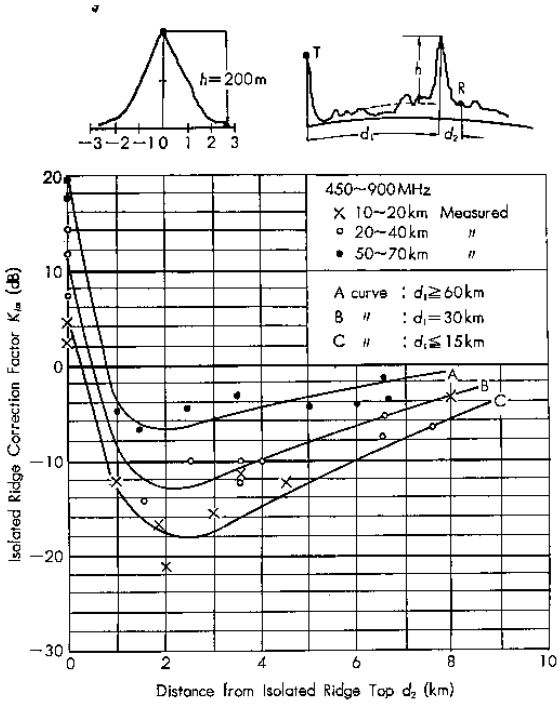

Fig. 31—Measured values and prediction curves for "isolated ridge correction factor" normalized at ridge height of $h=200$ m. For other ridge height, the conversion factor should be multiplied by factor of α shown in Fig. 32.

suffer any more than 1 dB even change with a change of 15~60 km in d_1. Take, for instance, Curve C at $d_1=15$ km and Curve A at $d_1=60$ km in Fig. 31 for the purpose of comparison. Although the tendencies relative to d_2 are very much alike, the relation between the two curves in their absolute value, differs according to the terrain factors relative to distances. It may be asserted then that, supposing there is a growth of terrain factors (or attenuation of the basic median referred to the free space value) in proportion to the distance, the correlation between Curves A, B, and C in Fig. 31 would again be formed here, if the correction factors obtainable from Curve K be arranged according to distances. This correlation might be taken as reasonable, aside from some minute differences in the absolute values of the curves in Fig. 31.

4.3 Correction Factor for General Slope of Terrain

In this section will be sought the relation of tne average angle of general slope on terrain θ_m to the correction factors in conformity to the definition given in Section 2.4, (1), (d).

Figure 34 shows, where the terrain is sloped for a distance of at least 5 to 10 km, the deviation of the measured median field strength from the basic median—or the slope terrain correction factor—in relation to the average angle of slope θ_m (in milliradian).

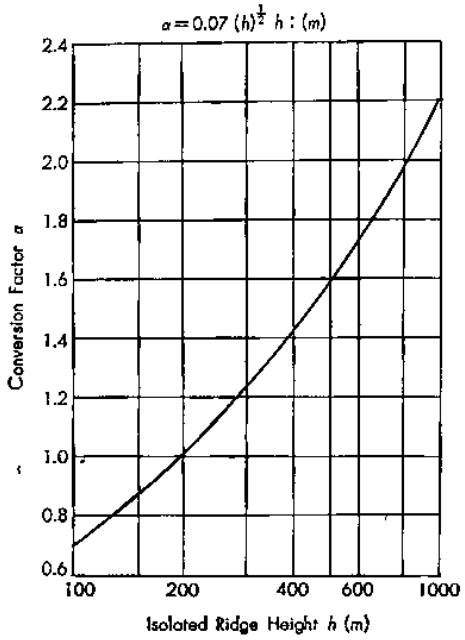

Fig. 32—Conversion factor to be multiplied to the value of Fig. 31, when ridge height $h \neq 200$ m.

The correction factor varies with the distance.

The curves are prediction curves drawn for some different distances; and curves for distances other than those may be obtained by interpolating the values of the known curves. Also, for the sloped rolling hilly terrain, the correction treated in Section 4.1 as well as this correction for general slope of terrain, will be made.

4.4 Correction Factor for Mixed Land-Sea Path

Where there is an expanse of sea or lake in the propagation path, the field strength is generally higher than on land only. There is an empirical method[17] of prediction in England which is based on experiments conducted on the North Sea.

This method may be convenient for the prediction of factors between one point and the other; but a large number of such factors will have to be managed in a very troublesome way, where there are various base station antennas propagating waves over a wide range of area, as in the case of mobile radio service.

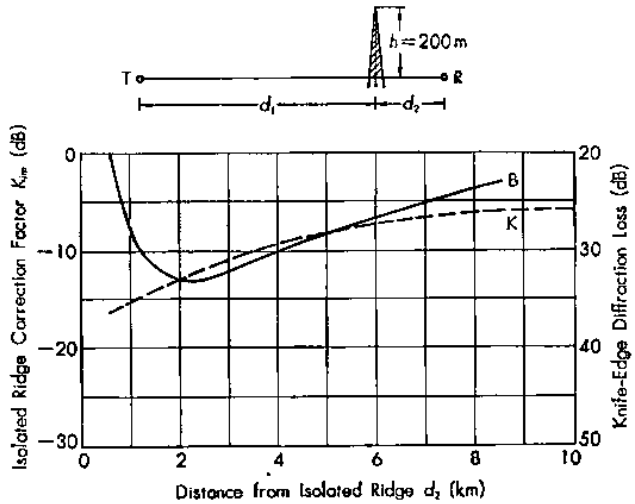

Fig. 33—Relation between the curves of Fig. 31 and of knife-edge diffraction loss. (450 MHz)

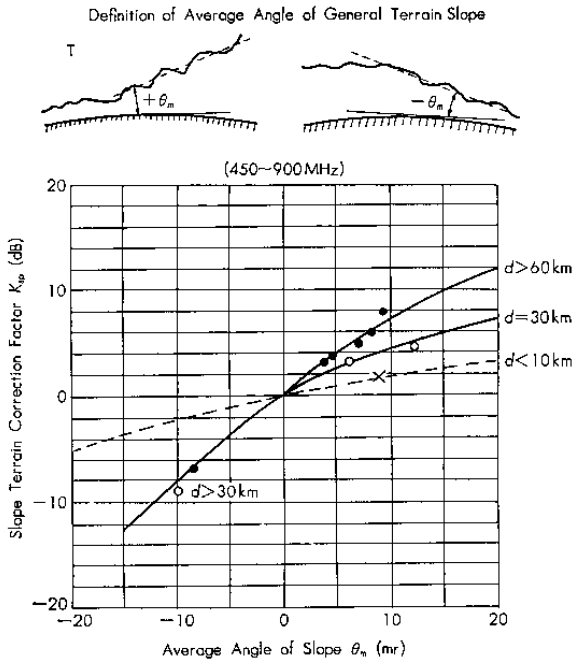

Fig. 34—Measured value and prediction curves for "slope terrain correction factor."

From a practical point of view, this method will turn to finding the relation between the distance parameter of mixed land-sea path (β), which is defined in Section 2.4, (1), (e), and a value called the correction factor for mixed land-sea path, that is, the deviation of the measured median field strength from the basic median.

Figure 35 shows the measured values for this correction factor as the distance varies and also as the expanse of water is near the vehicular or the base station. The degree of field strength rise (correction factor) is larger if the water adjoins the vehicular station (ppper diagram (A)) than if it adjoins the base station (pper diagram (B)), depending further on the distance. The full and the broken lines represent the prediction curves for (A) and (B), respectively. For distances other than indicated, curves may be obtained by interpolation. If the water is in the middle of the path (β to be found from Fig. 8(c)), the intermediate valnes of the full and broken line values will answer very well.

5 Location Variability

Among the propagation characteristics for land-mobile radios, location variability comes next in importance to attenuation, which has been described so far.

Let location variability be considered from the viewpoint of variations in the median level for a sampling interval on the one hand, and in the instantaneous level for a small sector in the same interval on the other.

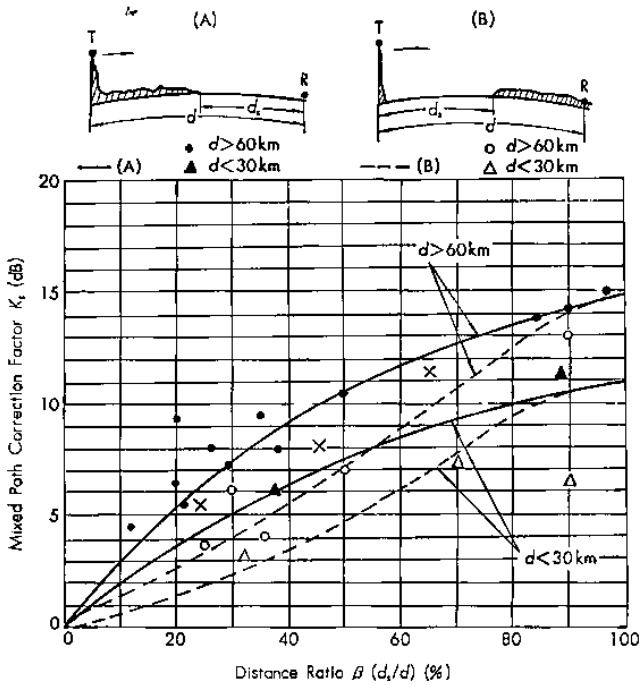

× When the sea lies in the middle of the path.

Fig. 35—Measured values and prediction curves for "mixed path correction factor."

5.1 Distribution Form of Field Strength

5.1.1 Distribution of Instantaneous Field Strength in Small Sector

As stated before, the variation in the instantaneous field strength level experienced by a mobile van station, is due to the fact that it crosses with such rapidity the standing waves which result from the multi-path reflected and diffracted waves. The form of distribution, as seen from its model, conforming to the Rayleigh distribution in this case, will be examined according to the situation of the existing obstacles.

Figure 36 shows, with its respective 50% values meeting together, the distribution of instantaneous field strength for a small sector of about 50 m, in an urban (a) and a forest (b) area, respectively, at different frequencies.

The curves are seen gathering along the Rayleigh distribution theoretical curves. It may be assumed that the variation speed increases but its depth (or the from of distribution) does not change in proportion to the speed of the mobile radio car.

Meanwhile, in a suburban area where obstacles present themselves intermittingly, rises often occur in the field strength; so the form of distribution tends to turn upward at its higher level side, resembling rather more the log-normal distribution than the Rayleigh distribution, and the standard deviation is about $\sigma = 6 \sim 7$ dB on the average.

5.1.2 Distribution of Small Sector Median in Sampling Interval

Even in an urban area where the obstacles are of similar kinds, the small sector median

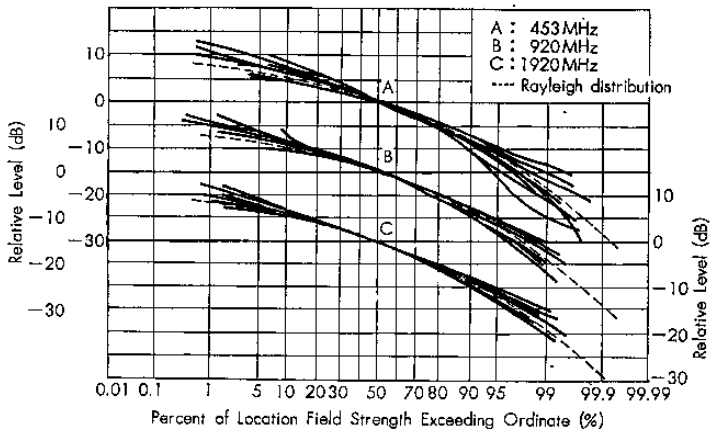

(a) In urban area (h_{te}=220 m, h_{re}=3 m)

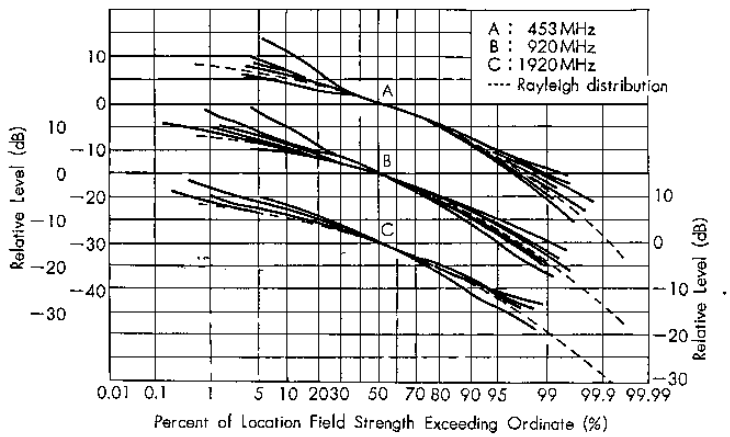

(b) In forest or behind forest (h_{te}=820 m, h_{re}=3 m)

Fig. 36—Examples of instantaneous field strength distribution in small-sector.

of instantaneous field strength referred to will change to a considerable degree, if the area or interval becomes wide.

Figure 37(a) shows an example of the cumulative distribution of median field strength for a small sector (about 20 m) in an urban sampling interval (1～1.5 km) at different frequencies. Here the curves mostly approximate the log-normal distribution.

Figure 37(b) shows a similar example of the distribution in a suburban area. The curves do not necessarily conform to the log-normal distribution influenced by obstacles, but they might, on the whole, be said to resemble it; and the standard deviation is usually larger than in an urban area.

On the basis of the foregoing description about the distribution form, consider how to

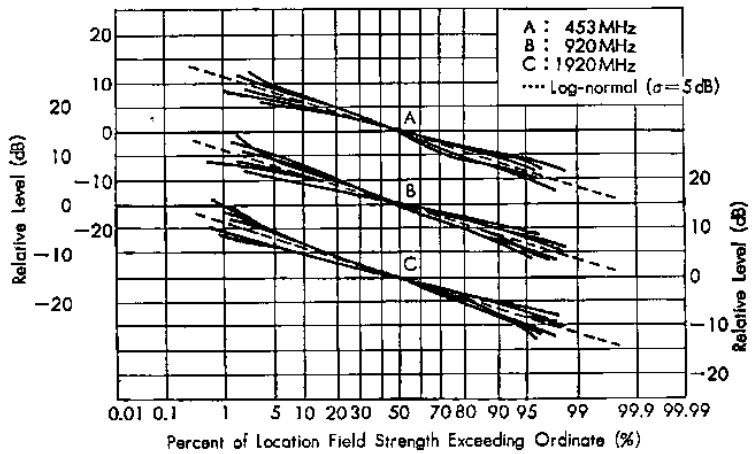

(a) In urban area (h_{te}=220 m, h_{re}=3 m)

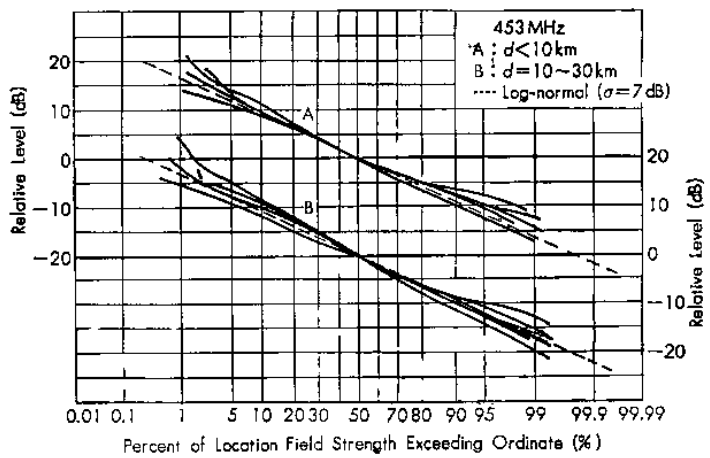

(b) In suburban area (h_{te}=60 m, h_{re}=3 m)

Fig. 37—Examples of distribution of small-sector median field in sampling inteval (1~1.5 km).

predict lacation variability.

5.2 Prediction of Location Variability

5.2.1 Prediction of Median Field Strength Location Variability

Figure 38 shows the measured mean values of standard deviation (σ) of small sector median field strength variation in an urban sampling interval, for classified distances of 1~3 km, 3~5 km, 20~30 km, and 70~80 km. The mean values of σ are not very closely connected with the base station antenna height or distance, but they become slightly larger at high frequencies.

The values of σ in a suburban and a rolling hilly terrain area, as may be known from

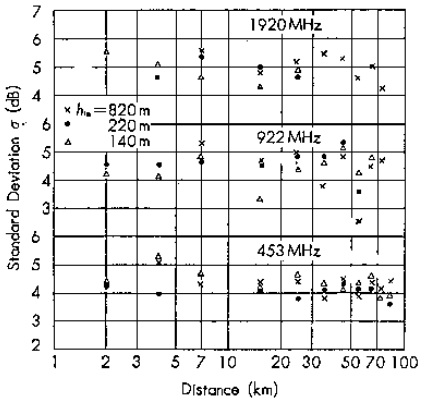

Fig. 38—Measured mean values of standard deviation of small-sector median field strength variation in urban area sampling interval (1~1.5 km).

Figs. 37 (a) and (b), are much larger than those for an urban area—about $\sigma \fallingdotseq 7$ dB—tending to grow large as the frequency increases.

For a wider region in which various obtacles peculiar to urban and suburban areas exist in a mixed condition, the small sector median distribution does not always take the log-normal distribution form according to how such obstacles are mixed, but is approximate to it if the obstacles are uniformly mixed.

In determining the extent of land for which location variability is to be used in the design of the land mobile service the size of interval or area traveled by the mobile radio car in a period of time taken for one telephone call, may become the accepted standard. With a mean holding time of one call to be 3 to 4 min, the travel speed of the car 60 km/hr, then the interval would come to 3~4 km and the area 2 km in radius.

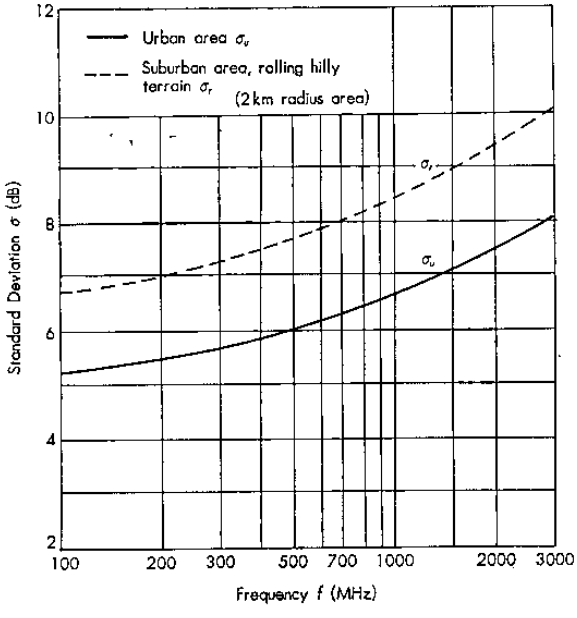

Fig. 39—Prediction curves for standard deviation of median field strength variation in urban, suburban and rolling hilly terrain.

The standard deviation σ of the median variability in an urban area in this respect, will be larger than that shown in Fig. 38. Figure 39 shows the prediction curves for standard deviations in urban, suburban, and rolling hilly terrain areas, each 2 km in radius.

5.2.2 Prediction of Instantaneous Field Strength Location Variability

(1) Prediction in Urban Area

The instantaneous variation of field strength in an urban small sector can be brougut near the Rayleigh distribution of such small-sector mediaps near the log-normal distribution which has standard deviation σ_u (in Fig. 39) in it. The overall variability, therefore, may be found from the theoretical composition of the two distribution functions. Figure 40 shows the prediction curves (in solid lines) for the instantaneous variation depths from the median field strength (V_{di}, 50～90%, 50～95%, 50～99% in depth) obtained from this composite distribution. Again the equivalent standard deviation where the composite distribution is nearly equal to the log-normal distribution (this is possible because of the large value of σ_u, if its small percentage is negligible) is expressed by σ_u in Fig. 40.

(2) Prodiction in Suburban Area and Rolling Hilly Terrain Area

The instantaneous variation of field strength

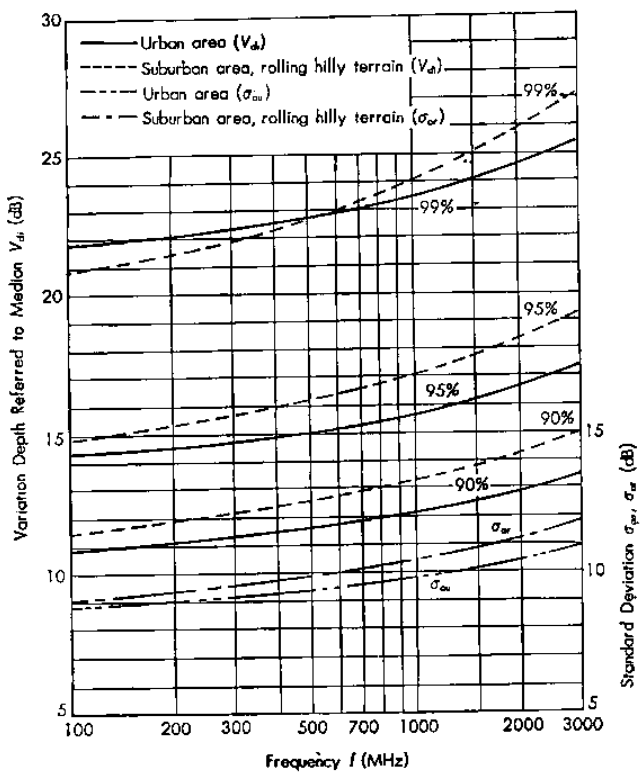

Fig. 40—Prediction curves for instantaneous variation depth from median field strength and standard deviation.

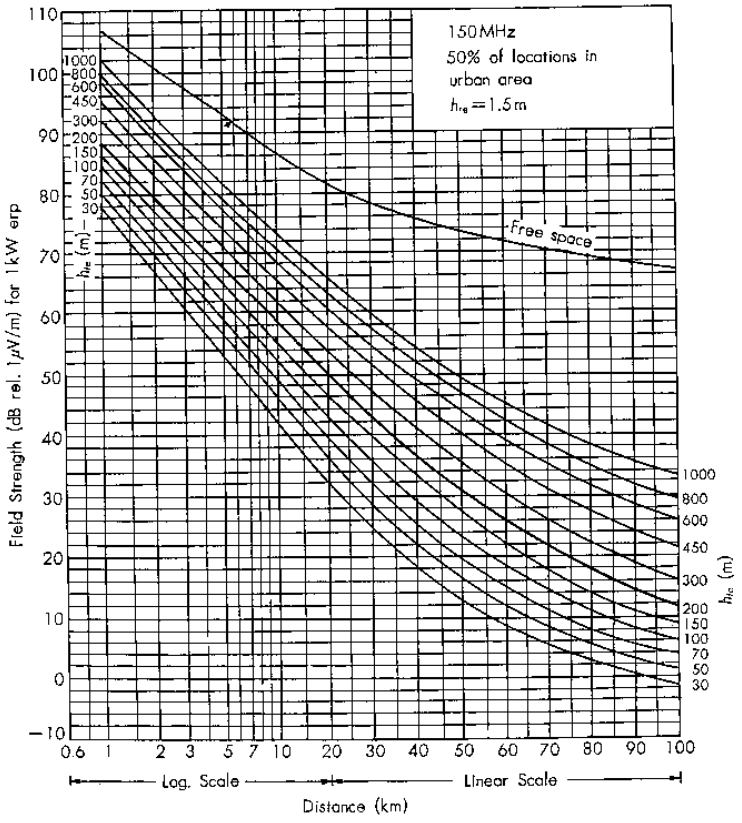

Fig. 41(a) 150 MHz Band

in a suburban and a rolling hill terrain area small sector, can, on the whole, approximate the log-normal distribution (where $\sigma=6$ B); and the distribution of such small sector medians to the long-normal distribution which has the standard deviation expressed by Curve σ_r in Fig. 39. From the composition of these two distributiohs may be found the overall distribution of instantaneous field strength in the area under examination.

Curve σ_r in Fig. 40 is the prediction curve for the standard deviation of this overall distriburion; and the curves in broken lines are for obtaining the variation depth V_{d1}.

6 Prediction of Field Strength; Comparison between Predicted and Measured Values

By making use of the various results and prediction curves so far examined, it is possible to obtain the field strength and its variability peculiar to areas of all sorts of terrain irregularities and environmental clutter usually met with.

6.1 Prediction Procedures

In this method of prediction, to obtain the basic median field strength in a qnasi-smooth terrain urban area is the starting

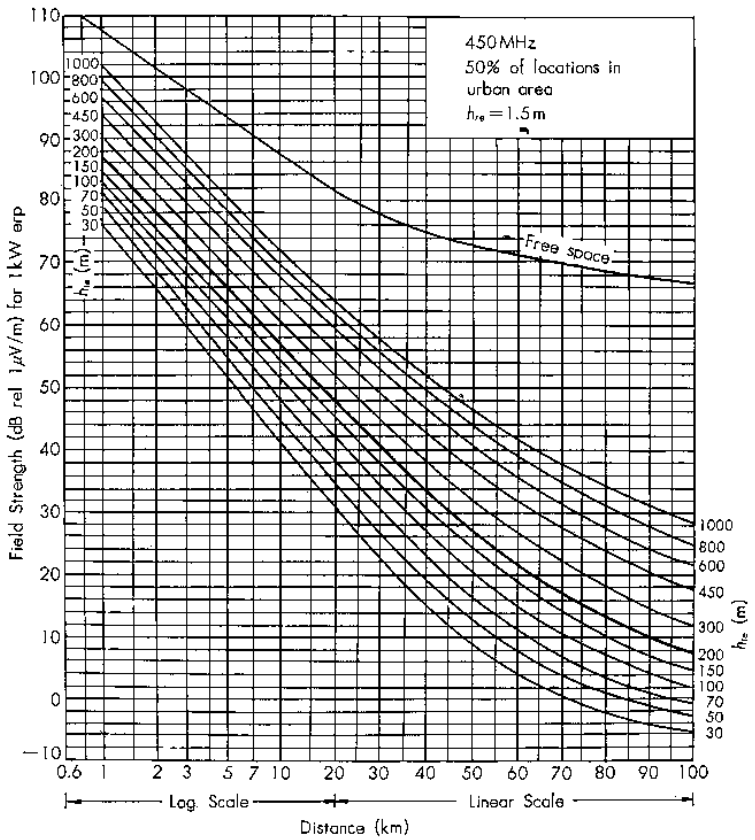

Fig. 41(b) 450 MHz Band

point. The prediction curves representing values for all those terrains and obstacles, are obtainable by adjusting the correction factors for the respective terrain parameters.

6.1.1 Prediction of Basic Median Field Strength (Curves)

The following equation (for addition and subtraction in dB) and curves are used for the prediction of the basic field strength median (curve) which is to be made the standard of prediction procedures:

$$E_{mu}=E_{fs}-A_{mu}(f, d)+H_{tu}(h_{te}, d)+H_{ru}(h_{re}, f) \quad (2)$$

where

E_{mu}: The median field strength (dB rel. 1μV/m) for a quasi-smooth terrain urban area under a given condition of transmission.

E_{fs}: The free-space field strength (dB real. 1μV/m) for a given condition of transmission.

$A_{mu}(f, d)$: The median attenuation relative to free space (basic median attenuation, dB) in an urban area, where the base station effective antenna height h_{te}= 200 m, vehicular station antenna height

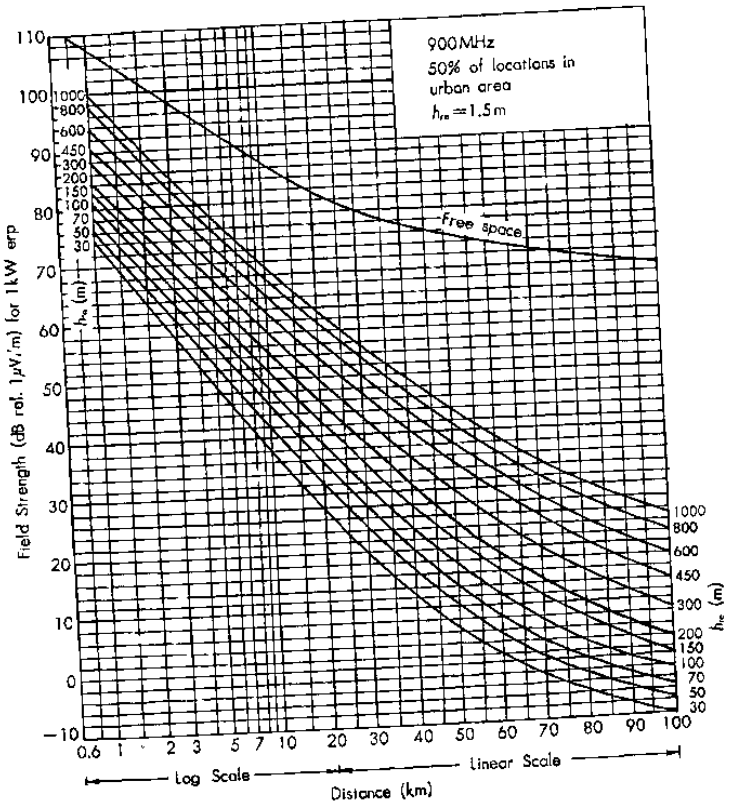

Fig. 41(c) 900 MHz Band

(above ground) h_{re}=3 m, expressed as a function of frequency and distance by the curves in Fig. 15.

$H_{tn}(h_{te}, d)$: The base station antenna height gain factor (dB) relating to h_{te}=200 m, expressed by the curves in Fig. 24 as a function of distance.

$H_{rn}(h_{re}, f)$: The vehicular station antenna height gain factor (dB) relating to h_{re} =3 m, expressed by the curves in Fig. 27 as a function of frequency.

Figures 41(a) to (d) show, respectively, at 150 MHz, 450 MHz, 900 MHz, and 1,500 MHz, the basic median field strength curves for the base station effective antenna height h_{te}=30, 50, 70, 100, 150, 200, 300, 450, 600, 800, and 1,000 m, when the effective radiation power P_{erp}=1kW, and the vehicular station antenna height h_{re}=1.5 m.

6.1.2 Drawing Field Strength Contour Curves over a Service Area

The procedures to follow in drawing the field strength contour curves around a base station are given below:

(1) Draw a terrain profile for eaeh proper azimuth angle, in order to obtain the base station effective antenna height h_{te} and terrain parameters of all sorts. (See Figs. 4 to 8.)

(2) Draw on a map, with the site of the

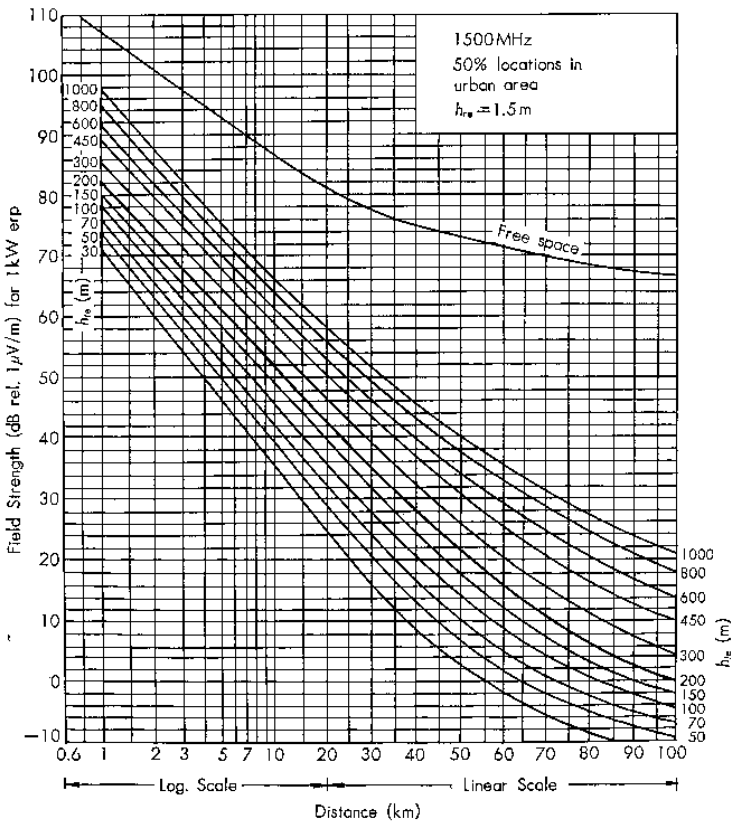

Fig. 41(d) 1500 MHz Band

Fig. 41—Prediction curves of "basic median field strength" (in urban area over the quasi-smooth terrain).

base station as their center and having regard to the height h_{te} fixed in (1), a certain number of basic median concentric circles (together with entry of their respective values), at intervals of metric lengths corresponding to 5 dB of the basic median field strength found from Section 6.1.1.

(3) Amend the basic median concentric circles according to the irregular terrain situation (quasi-smooth terrain excepted) and environmental clutter surroundings, by modifying the distances which correspond to the correction factors cited below:

(a) "Correction to the orientation of an urban area street"—correction factor ($+K_{at}$ dB) represented by Curve (a) in Fig. 18, if there are a large number of along-the-path streets in the area; and factor ($+K_{ac}$ dB) represented by Curve (b) in Fig. 18, if there are plenty of across-the-path streets.

(b) "Correction for a suburban area"—correction factor ($+K_{mr}$ dB) shown in Fig. 20, if the area abounds in suburban features.

(c) "Correction for an open area"—the correction factors ($+Q_0$, or $+Q_r$ dB) shown in Fig. 22 in the open area on a quasi-smooth

terrain, according to the degree of shielding.

(d) "Correction for a slope terrain"—correction factor ($+K_{sp}$ dB) shown in Fig. 34 in an area where the ground is sloped up or down for a distance of at least 5～10 km.

(e) "Correction for a mixed land-see path"—correction factor ($+K$, dB) represented by Curve (A) or (B) in Fig. 35, where there is an expanse of sea or lake in the propagation path.

(f) "Correction for a rolling hilly terrain"—correction factor ($+K_h$ dB) in Fig. 28 on an undulating hilly terrain.

(g) "Fine correction for a rolling hilly terrain"—fine correction factor ($\pm K_{hf}$ dB) in Fig. 29, where there are many roads running

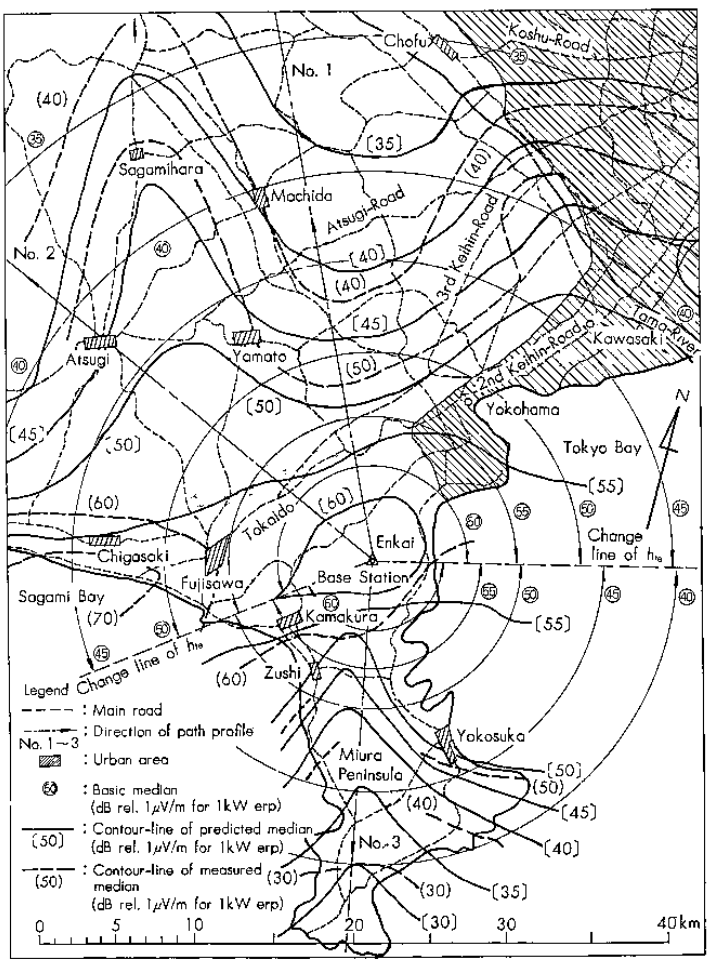

Fig. 42—Comparison of contour line for predicted median field strength with that of measured median in broad area. (Base station: Enkai, f=450 MHz)

on the tops or bottoms of hills.

(h) "Correction for an isolated ridge"—correction factor ($+K_{im}$ dB) shown in Figs. 31 and 32, on top of or behind a ridge that lies in the propagation path. This correction is made when the ridge resembles the model shown in the upper left-hand margin of Fig. 31; but the maximum value of correction show in the same diagram would probably appear at the foot of the ridge, when its breadth is different from that of the model.

6.2 Comparison between Prediction Values and Measured of Field Strength

In this section a comparison will be made between the field strength vs. distance curves obtainable from the diagrams and predication methods cited in the preceding section on the one hand, and representative propagation curves hitherto reported on the other, in order that the reliability of the propagation design data suggested by this paper may be confirmed.

(1) Example of A Given Broad Area

Figure 42 shows a comparison between the measured and the predicted curves of the equifield strength for that part of the Kanto district which includes the Miura peninsula and the Tama highlly zone, with the base station (microwave relay station) established at Enkai. The frequency used is 450 MHz and the base station antenna height is 183 m

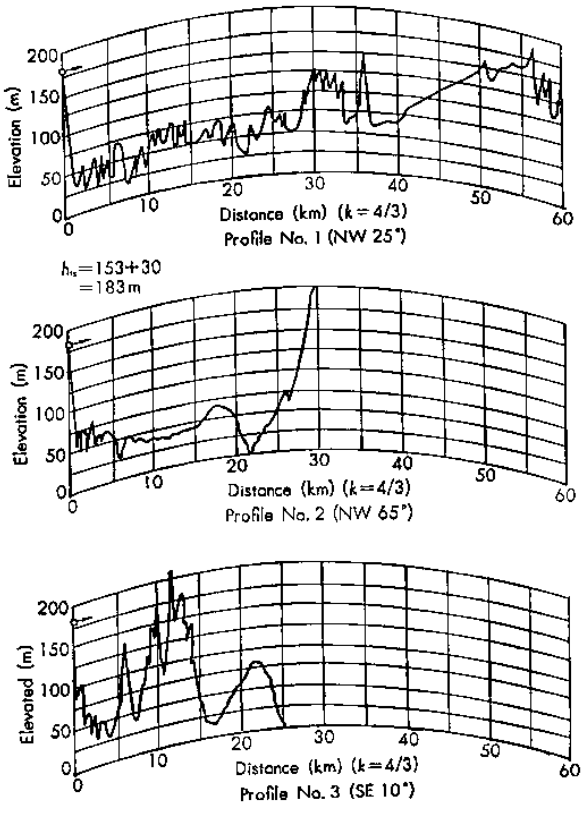

Fig. 43—Path profile on representative direction from Enkai base station.

above sea level. The equifield strength measured is drawn from the data collected by vehicular stations while running on the principal roads; and the prediction curves follow the method mentioned in Section 6.1.2. Figure 43 shows the representative path profiles in this area along three different directions from the base station, as indicated in Fig. 42 as No. 1~No. 3. They suggest that this area may be divided into two parts—the base station effective antenna height for one is 133 m and for the other it is 83 meters. The prediction equifield strength curves in Fig. 42 are drawn according to this distinction; only the rolling hilly part of the area dispenses with the process of fine correction referred to in Fig. 29. From the above, it may be conjectured that the predicted and the measured curves are in substantial agreement.

(2) Example of A Given Terrain Profile

Figure 44 shows a comparison between the measured field strength for the sampling interval on the propagation path whose profile is given in the lower diagram, and the prediction curves obtained by following the procedure of Section 6.1.2. The measured and the prediction curve are seen to correspond fairly well with each other.

(3) Comparisom of Prediction Curves with Measured Values by Other Institutions

The measurement data taken up for this comparison collected by other institutions, are partly intended for TV broadcasting. Where the receiving antenna is high, prediction is made through correction by means of the curves in Fig. 27.

The principal test data furnished are from the NHK Technical Laboratory,[8] Bell Telephone Laboratories,[4] and RCA.[18] Figures 45 to 47 show some of the results of comparison of these data. The frequencies and transmitting and receiving effective antenna heights are indicated in each diagram.

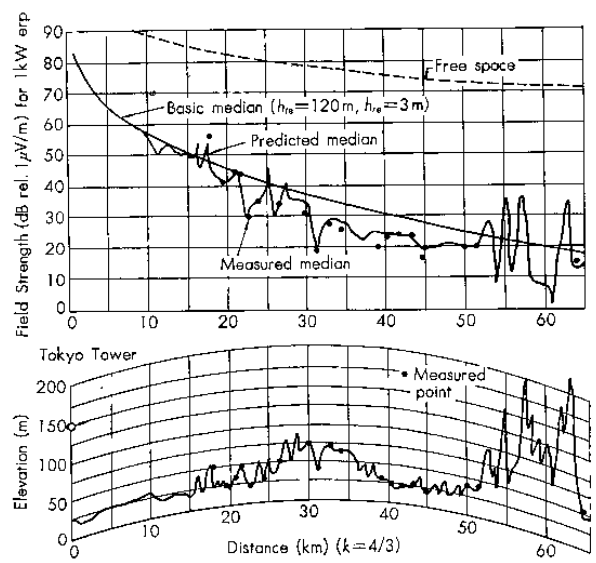

Ffg. 44—Comparison of measured and predicted median field strength on 55° SW radial from Tokyo Tower. (h_{te}=120 m, h_{re}=3 m, 453 MHz)

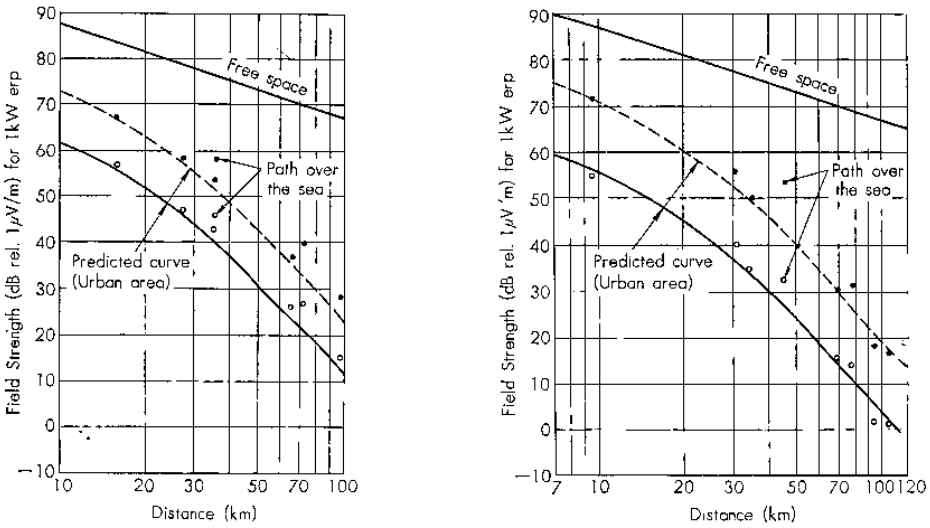

(a) ●; f = 176 MHz h_{te} = 140 m, h_{re} = 10 m
○; 〃 〃 , h_{re} = 4 m

(b) ●; f = 670 MHz h_{te} = 100 m, h_{re} = 10 m
○; 〃 〃 , h_{re} = 4 m

Fig. 45—Comparisons of NHK's data with predicted median field strength curves (urban area).

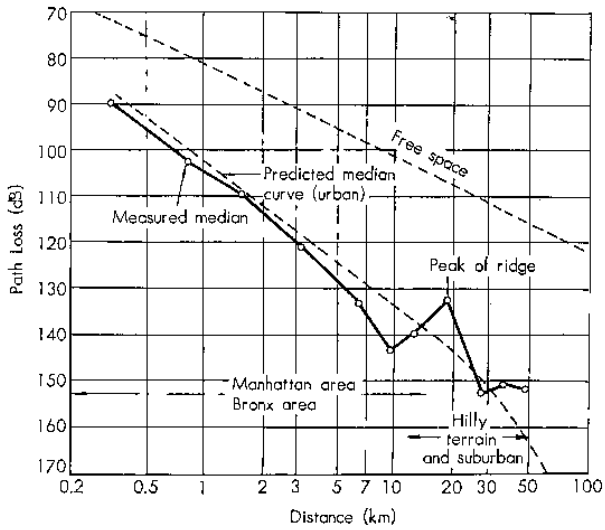

(a) ○; f = 450MHz median, h_{te} = 137 m, $h_{re} \fallingdotseq$ 3 m

Fig. 46

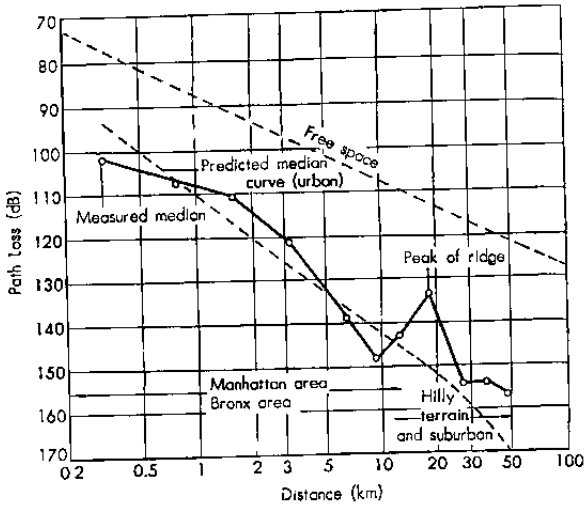

(b) ○; f=900 MHz Median, h_{te}=137 m, h_{re}≒3 m

Fig. 46—Comparisons of Bell Laboratories' data with predicted median field strength curves.

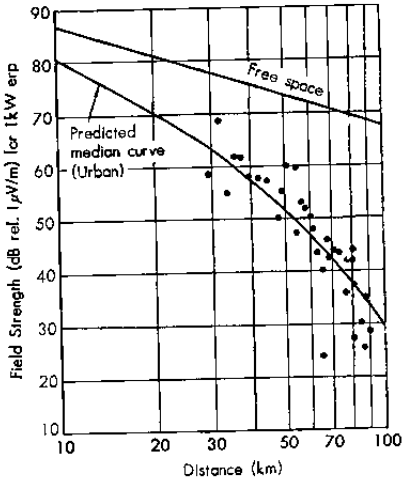

Fig. 47—Comparison of RCA's data with predicted median field strength curve.

The NHK data (Fig. 45) is connected with medium and small cities, showing the median of the measurements taken at about twenty fixed points per city. With the exception of the cities where there are land-sea paths, the distane characteristics tend to be almost the same as those for the prediction curves. The Bell data (Fig. 46) provide us with two medians—one of short-distance values measured at the lofty-building area of Manhattan, and the other of those measured along several directions for a distance of 10 km or more, at suburban and hilly terrain areas. As nothing is known about the suburban and hilly terrain irregularities and environmental clutter along the whole route, correction is impossible to make on the values; but, judging from the urban prediction curves, there is a general agreement on distance characteristics between the measured values and prediction curves.

The RCA data in Fig. 47 show the results for a comparatively smooth terrain area. Here again, there is also a fair agreement.

(4) Comparison between Representative

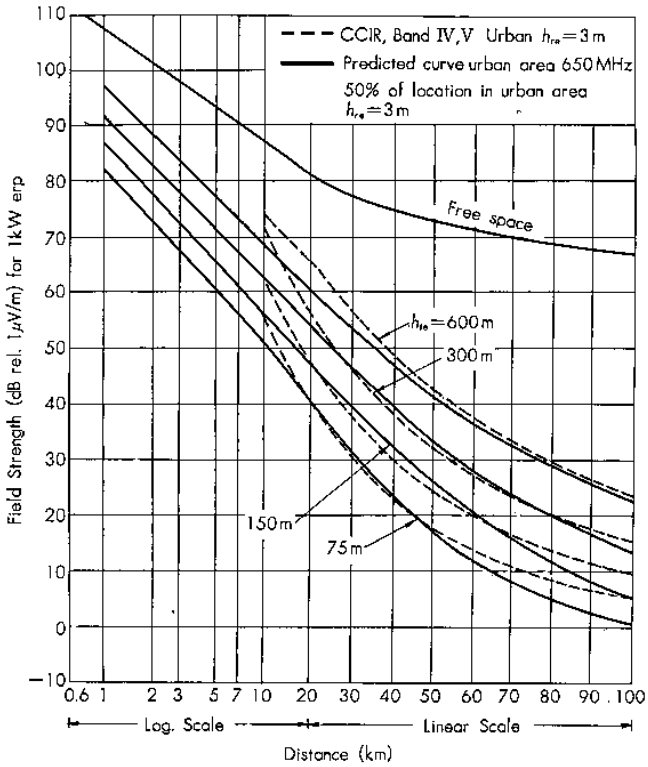

Fig. 48—Comparison of CCIR propagation curves with predicted curves.

Propapation Curves and Prediction Curves.

Considering the importance of land-mobile radio service, CCIR has recently reported[5] the antenna height (3m) gain correction factor in urban and suburban areas found from the former propagation curves (Rec. 370-1). As a representative case, let the urban field strength curves obtainable therefrom be taken up and compared with the prediction curves.

The curves in broken lines in Fig. 48 represent the propagation curves in the urban area for a 3 m high vehicular station antenna, drawn on correcting the curves of Rec. 370-1 by means of the correction factors for Band IV and V shown in Rep. 239-1. Those in solid lines represent the prediction curves at 650 MHz, or the center frequency of Band IV and V 450~1,000 MHz. Here a batter agreement exists for a distance of 20~60km; but, where the distance is below 20 km, or where the antenna is low and the distance is 60 km or more, the CCIR curves result in rise above the prediction curves, so that further study would be necessary with respect, especially, to long-distance characteristics.

7 Conclusion

For the description given so far, various characteristics about VHF and UHF land-mobile radio service, hitherto ambiguous in this as well as foreign countries, have become clarified; and simple and practical methods of drawing prediction curves been established for obtaining the field strength which is open to much-complicated location variability. This has also made it practical in land-mobile radio service to connect circuit reliability with

site location, suggesting a guiding principle to the development of new frequency bands in the future. However, the intricacy of propagation characteristics has not entirely been elucidated by this paper. Also, the test data on correction factors for irregular terrains cannot be said to be sufficient. In order to solve these problems, there is no other way than to rely upon future research.

In concluding this paper, the authors wish to express their sincere thanks to Mr. T. Kamiya, formerly Director of Transmission System Development Division, Mr. F. Iwai, formerly Staff Engineer (now in Fujitsu Co., Ltd.), Dr. T. Masuda, formerly Chief of Radio Transmission Section, Dr. T. Morinaga, Chief of Mobile Radio Section for their deep understanding and invaluable guidance; and also to other persons who shared this study for their efforts in conducting the experiments.

References

(1) CCIR; Rec. 370-1, Oslo, 1966, II, p. 24.
(2) P. L. Rice: Troposheric Fields and their Long-Term Variability as Reporded by TASO, *Proc. IRE.*, **48**, 6, p. 1021, June 1960.
(3) J. J. Egli; Radio Propagation above 40 MC over Irregular Terrain, *Proc. IRE.*, **45**, 10, p. 1383, Oct. 1957.
(4) W. E. Young: Comparison of Mobile Radio Transmission at 150, 450, 900 and 37000 MC, *BSTJ.*, 31, 6, p. 1008, Nov. 1952.
(5) CCIR: Rep. 239-1, Oslo, 1966, **II**, p. 125.
(6) E. Shimizu and T. Morinaga, et al.; Propagation Tests of Frequencies for VHF Mobile Radio, *Report of E.C.L.*, NTT, **5**, 1, p. 13, Jan. 1957.
(7) CCIR Doc.; Resuls of Propation Measurements in Large Cities, Doc. V/99-E, p. 21, Jan. 1966 (Italy).
(8) I. Murakami and E. Sugiyama, et al.: Screening Effect of Medium-Sized and Small Cities on UHF and VHF Propagation, *NHK Tech. Journ.*, **13**, 2, p. 12, Mar. 1961.
(9) CCIR: Rep. 239-1. Oslo, 1966, **II**, p. 123.
(10) A. Kinase and K. Suga: Influence of Buit-up City Situation on Propagation Characteristics of UHF Band, *NHK Tech. Journ.*, **19**, 6, 1967.
(11) CCIR: Rec. 370-1, Olso, 1966, **II**, p. 25.
(12) A. Lagron; Forecasting Television Service Field, *Proc. IRE.*, **48**, 6, p. 1009, June, 1960.
(13) CCIR, Doc.; Correction Factor for the Frequency Band, I-V, Doc. V/28-E, p. 22, 1965, (P. P. of Poland).
(14) F. H. Wise: The Influence of Propagation Factors on UHF Television Broadcasting, *Telev. Soc. Journ.*, **10**, 11, p. 330, Nov. 1964.
(15) T. T. Goldsmith, et al.: A Field Survey of Television Channel 5 Propagation of New York Metropolitan Area, *Proc. IRE.*, **37**, 5, p. 556, May 1949.
(16) T. Esptein et al.; An Experimental Study of Wave Propagation at 850 MC, *Prock. IRE.*, **41**, 5, p. 595, May, 1953.
(17) E. Sofer, et al.; Tropospheric Radio Wave Propagation over Mixed Land and Sea Paths., *Proc. IEE.*, **113**, 8, p. 1291, Aug. 1966.
(18) D. W. Peterson: Comparativè Studyof Low-VHF, High-VHF and UHF Television Broadcasting in the New York City Area, *RCA Rev.*, **24**, 1, p. 57, Mar., 1963.

* * * *